Chapter 5

Post-combustion capture of CO_2 using novel aqueous Triethylenetetramine and 2-Dimethylaminoethanol amine blend: Equilibrium CO_2 loading-empirical model and optimization, CO_2 desorption, absorption heat, and ^{13}C NMR analysis

Abstract

The equilibrium CO_2 loading was estimated by absorption of CO_2 gas in the bubble column reactor for a novel aqueous amine blend of Triethylenetetramine (TETA) and 2-Dimethylaminoethanol (DMAE). The absorption study was performed at a temperature of 298.15 to 333.15 K, mole fraction of TETA from 0.05 to 0.2, solution concentration varied from 1 to 3 mol/L, and CO_2 partial pressure ranging from 10.13 to 25.33 kPa. The maximum experimental equilibrium CO_2 loading was 0.92 mol CO_2/mol amine at 315.65 K temperature, 17.73 kPa CO_2 partial pressure, 0.13 mole fraction of TETA, and 1 mol/L solution concentration. The absorption results were validated by an empirical model with an average absolute relative deviation of 5.631 %. The desorption study was performed at a constant temperature and pressure of 393.15 K and 17.73 kPa, respectively. The cyclic loading capacity of this blend at 3 mol/L concentration showed 55.03 % higher results than that of 30 wt% (5 mol/L) monoethanolamine (MEA). The Gibbs-Helmholtz equation calculated the heat of CO_2 absorption, and for this amine blend, it was found to be -67.135

KJ/mol. ^{13}C nuclear magnetic resonance (NMR) spectroscopy was adopted to identify the chemical species in CO_2-loaded and unloaded amine blends. Response surface methodology software optimized the final response. It predicted optimal equilibrium CO_2 loading of 0.926207 mol CO_2/mol amine at 304.36 K temperature, 0.14 mole fraction of TETA, 17.24 kPa partial pressure of CO_2, and 1 mol/L solution concentration.

5.1 Introduction

In the current scenario, the country's population is rapidly increasing, and in order to meet their basic needs, humans are putting an additional strain on the earth's climatic conditions. Greenhouse gas emissions are blameworthy for global warming, which is a key problem for the entire world. Anthropogenic carbon dioxide (CO_2) emissions from the combustion of conventional fossil fuels destabilize the earth's atmospheric conditions by raising its temperature [1-9]. According to the Intergovernmental Panel on Climate Change (IPCC) report, if the CO_2 emission rate cannot be restricted effectively, then by the year 2100, there will be a temperature rise of 2 ℃ [2,10-12]. This situation would result in a 3.8 m rise in sea water level, drought, flooding, frequent heat waves, storms, and other natural disasters [1,12]. The primary sectors that handle CO_2 emissions are cement, aluminium, iron and steel, petrochemical, thermal power plants, and a variety of other chemical-based industries [2,5,13]. Among them, coal-fired thermal power plants contribute the highest CO_2 emission into the atmosphere [8].

Carbon capture and its storage (CCS) is the most promising way to mitigate CO_2 emissions to a large extent [6,13-16]. CCS employs three primary techniques: pre, post, and oxy-combustion [2,6,11]. CO_2 can be captured using various methods such as absorption, adsorption, membrane separation, chemical looping combustion, cryogenic separation, and

the microalgae process [1-3,8,17-18]. However, post-combustion CO_2 capture from the coal-fired thermal power plant relies on absorption by aqueous amine scrubbing. It has been the most well-established and versatile method used for so many decades [1-5,7,16,19-23]. Many traditional aqueous amines, such as Monoethanolamine (MEA), Methyldiethanolamine (MDEA), Diethanolamine (DEA), 2-Amino-2-methyl-1-propanol (AMP), and Piperazine (PZ), are used to capture CO_2 [2,3,6,8,13,15,19-20]. MEA has been used for CO_2 capture for a long time and is regarded as a benchmark [14,16,18-19]. Their massive demand for regeneration energy and scanty CO_2 solubility has influenced the researchers to work on various amine blends. Primary and secondary amines are high kinetics solvents and are referred to as activators ($\Delta H_{abs} \approx 80$ kJ/mol CO_2), while tertiary or hindered amines are low kinetics solvents are known as promoters ($\Delta H_{abs} \approx 60$ kJ/mol CO_2) [1,11,24-25]. Activators form carbamates, while promoters produce bicarbonates in reaction to CO_2. The heats of absorption of activators are more than promoters. It simply means that the energy requirement for breaking off the carbamates is greater than bicarbonates [20]. Based on the experimental analyses, most of the literature concluded that the regeneration energy cost is 70–80% of the entire operational cost [11,15,20,25-27]. Activators have disadvantages such as high regeneration energy demand, low absorption capacity, equipment degradation, corrosiveness, etc. On the other hand, tertiary amines have a higher CO_2 absorption capacity and a lower regeneration energy requirement [4-6,15,22]. Therefore, amine blending, i.e., a concoction of activators with promoters, enhances the overall property of the amine blend and simultaneously causes a tremendous reduction in regeneration energy [28].

TETA is a polyamine that contains two primary and two secondary amino groups present in its chemical structure [29-33]. Therefore, TETA has four reactive sites on which CO_2 can make a very effective chemical reaction. TETA on reaction with CO_2 has a high absorption rate, fast reaction kinetics, and large equilibrium CO_2 loading, but it has low regeneration efficiency [31-32,33-34]. Leu et al. [30] studied the aqueous behavior of TETA+H_2O to capture CO_2 and discovered a fantastic equilibrium CO_2 loading of 1.062 mol CO_2/mol amine. Luo et al. [29] targeted the equilibrium CO_2 loading and cyclic capacity of MEA and TETA. They concluded that TETA produced the best results, and the heat of absorption of TETA was slightly lower than that of conventional MEA. Ramezani et al. [32] prepared the aqueous blend of K_2CO_3+TETA, and the CO_2 absorption was performed in the stirred cell reactor. Experimental results revealed that the absorption capacity of the K_2CO_3+TETA solution was higher than MEA. The absorption capacity increased with an increase in mole fraction of TETA and decreased with high temperature.

DMAE is a novel tertiary amine that is easily produced from renewable resources and has the potential to replace the majority of tertiary amines [15,21]. This tertiary amine has good degradation resistance, a low regeneration energy demand, and a high CO_2 loading capacity [5,22]. Chowdhury et al. [4], concluded that DMAE has tremendous CO_2 absorption capacity compared with conventional MDEA. As a result, the aqueous amine blend of TETA and DMAE could be used to capture CO_2 by utilizing the individual properties of TETA and DMAE.

It is essential to examine the intermediate complexes of the species formed while reacting with CO_2. The chemical species of the aqueous amine blend of TETA+DMAE were identified using ^{13}C NMR spectroscopy [36-45]. Response surface methodology

(RSM) software can optimize any type of engineering or non-engineering problem. Any experimental work can be correlated either by first or second-order regression models [46], and central composite design (CCD) or box-behnken designs (BBD) are helpful to optimize any task [47-48]. In their optimization work, Nuchitprasittichai et al. [40], Sahraie et al. [49], Hemmati et al. [50], and Nuchitpraittichai et al. [51] accepted BBD analysis. Whereas CCD investigations were done by Gil et al. [52], Song et al. [53], Das et al. [54], Saeidi et al. [55], and Asgarifard et al. [56].

This present work studied the absorption and desorption behavior of a novel aqueous amine blend of TETA+DMAE. An empirical model was developed to validate the absorption results, and the heat of CO_2 absorption was also estimated by using the Gibbs-Helmholtz equation. The effect of temperature, mole fraction of TETA, solution concentration, and CO_2 partial pressure on equilibrium CO_2 loading was evaluated. The reaction mechanism of TETA and DMAE with CO_2 was suggested, and the species identification was made by ^{13}C NMR spectroscopy. The equilibrium CO_2 loading was optimized using RSM software at different independent variables involved in the entire system.

5.2 Materials and methods

5.2.1 Chemicals and equipment used

The TETA (purity ≥ 97%) and DMAE (purity ≥ 99%) amine chemicals were purchased from the Sisco Research Laboratories (SRL) Private Limited, India. The aqueous amine blend of TETA+DMAE with different concentrations was used as a CO_2 absorption medium. MEA (purity ≥ 98%) was used as a benchmark for comparing results and validating the experimental setup, and it was procured from Sd Fine Chemical, India. HCl

(purity = 35–38%) and D_2O (purity = 99%) were acquired from Merk, Germany. Equilibrium CO_2 loading was estimated with the help of the HCl titration method, and D_2O was used as a signal lock in the NMR analysis. Pure N_2 and CO_2 gas cylinders (99.99% purity each) were purchased from Linde India Limited, and the flow rate of these gases was controlled by digital mass flow controllers, which were provided by Alicat Scientific, India (Model No.- MC-500SCCM-D-DB9M, $\pm$ 0.32 % reading or $\pm$ 0.02 % full scale). Descriptions of all the chemicals with their significant properties are listed in Table 5.1. CO_2 gas concentration in the simulated gaseous mixture was judged with the help of a portable infrared-based CO_2 gas analyzer (Serial no. A-0191 (PM), Gasboard–3800P, Software version–1606.25, CO_2 range: 0–100 %v/v). Double-distilled water was prepared on the laboratory scale, and the same was used during the entire experiments.

Table 5.1 Specification of chemicals, along with their significant properties used in this experimental work.

Chemical used	CAS Number	Structure	BP (℃)	ρ (Kg/m^3)	Molecular weight (g/mol)	Initial purity	Source	Purification method
Triethylenetetramine (TETA)	112-24-3	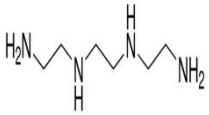	266.6	982	146.238	≥97%	SRL Private limited, India	None
2-Dimethylaminoethanol (DMAE)	108-01-0	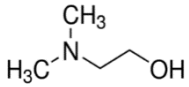	134.1	890	89.138	≥99%	SRL Private limited, India	None
Monoethanolamine (MEA)	141-43-5	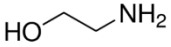	170	1011.7	61.08	≥98%	Sd Fine chemical limited, India	None
Hydrochloric acid (HCL)	7647-01-0	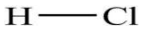	-85.05	1200	36.46	35–38%	Merck, Germany	None
Carbon dioxide gas (CO_2)	124-38-9	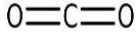	-78.46	1.98	44.01	99.99%	Linde India limited	None
Nitrogen gas (N_2)	7727-37-9	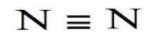	-195.8	1.25	14.00	99.99%	Linde India limited	None
Deuterium oxide (D_20)	7789-20-0	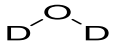	101	1104	20.03	99.9%	Merk, Germany	None
Distilled Water (H_2O)	7732-18-5	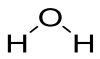	100	998.2	18.02	99.9%	Prepared at lab scale	Double distillation

5.2.2 Description of the experimental setup

The working of the CO_2 capture apparatus can be understood in the three major sections, i.e., (1) preparation of CO_2 simulated gas mixture, (2) achievement of the desired composition of CO_2 gaseous mixture, and (3) absorption and analysis of simulated CO_2 gas in the amine-based physical solvent. A detailed description of the CO_2 absorption experimental setup has already been provided in Section 3.2.3 of Chapter 3.

5.2.3 CO_2 absorption investigation

The experimental runs were performed at atmospheric pressure, the temperature range of 298.15–333.15 K, 0.05–0.20 mole fraction of TETA (activator), solution concentration varied from 1–3 mol/L, and partial pressure varied in the range of 10.13–25.33 kPa. At different operating conditions, the simulated CO_2 gaseous mixture was absorbed in the aqueous amine blend mixture of TETA+DMAE. Response surface methodology (RSM) software and some separate experimental runs at various operating conditions generated the entire operational sets of this experimental work. RSM software (Trial version) automatically generated experimental sets under various operating conditions. Some of the experimental sets, on the other hand, were generated separately to get the correlations between the independent variables. The complete schematic representation of the CO_2 absorption setup is already shown in Figure 3.1. The volume of water displaced during titration indicates the volume of CO_2 dissolved, and the volumetric method is helpful for its calculation (Equilibrium CO_2 loading - By Eq. 5.1) [2,57]. Absorption capacity calculation was obtained by using Eq. 5.2.

$$\alpha = 12.1942 \times \frac{V_{CO_2}}{C_{blend} \times V_{CO_2\ saturated}} \times \frac{1}{(273.15+T)}\ ;\ \text{mol } CO_2/\text{mol amine} \quad (5.1)$$

$$\text{Absorption capacity} = \alpha.C_{blend};\ \text{mol } CO_2/\text{L Solution} \quad (5.2)$$

Where α denotes equilibrium CO_2 loading and V_{CO2}, C_{blend}, $V_{CO2\ saturated}$, T are the volume of CO_2 gas released (L) from the amine solution, amine blend concentration (mol/L), volume of CO_2 saturated amine sample (L), and room temperature (℃), respectively.

5.2.4 CO_2 desorption investigation

The complete description of the CO_2 desorption experimental setup and its schematic representation have already been provided in section 3.2.5 and Figure 3.2 of Chapter 3, respectively. Cyclic equilibrium CO_2 loading and cyclic capacity were calculated by using Eq. (5.3) and Eq. (5.4), respectively.

$$\Delta\alpha = \alpha_{315.65k,17.73kPa} - \alpha_{393.15k,17.73kPa}\ ;\ \text{mol } CO_2\text{/mol amine} \quad (5.3)$$

$$\text{Cyclic capacity} = \Delta\alpha.C_{blend};\ \text{mol } CO_2\text{/L Solution} \quad (5.4)$$

5.2.5 Heat of CO_2 absorption (ΔH_{abs})

The heat of absorption of nearly 3 molar aqueous amine blend solution of TETA+DMAE was estimated only after calculating the equilibrium CO_2 loading of this aqueous amine blend at different temperatures (T) and CO_2 partial pressures (P_{CO2}). The temperature varied from 298.15 to 333.15 K, and the CO_2 partial pressure changed from 10.13 to 25.33 kPa. The heat of absorption was calculated by using the Gibbs-Helmholtz equation [45,57-60], and it is represented by Eq. 5.5.

$$\frac{d(\ln(P_{CO2}))}{d(\frac{1}{T})} = \frac{\Delta H_{abs}}{R} \quad (5.5)$$

Where $P_{CO2,}$T, ΔH_{abs}, and R are partial pressure of CO_2 (kPa), temperature (K), heat of absorption (J/mol), and universal gas constant (J/mol.K), respectively. The value of ΔH_{abs} was calculated by multiplying the slope of the graph in between $\ln(P_{CO2})$ vs. $(\frac{1}{T})$ and the

universal gas constant (R). Various data sets of (P_{CO2}) and ($\frac{1}{T}$) were selected for similar equilibrium CO_2 loading.

5.2.6 Response surface methodology (RSM) - statistical optimization approach

CCD was selected to optimize the equilibrium CO_2 loading of this experimental work. Temperature (T), mole fraction of TETA (m_{TETA}), partial pressure of CO_2 (P_{CO2}), and solution concentration (C) were the independent variables, and the final response was the equilibrium CO_2 loading (α_{exp}). Design expert software of trial version 8.0.6 was used to create the run samples at different operating conditions, and a total of 30 runs were obtained with six central points. The limits of the independent variables that were inserted in the software to generate the entire run sheet were T = 298.15–333.15 K, m_{TETA} = 0.05–0.20, C = 1–3 mol/L, and P_{CO2} = 10.13–25.33 kPa. The analysis of variance (ANOVA) with a lack-of-fit test was checked to validate the results or model fitness of the applied model. The theoretical information associated with designing of experimental run sets from RSM has already been discussed in Section 3.2.9 of Chapter 3.

5.3 Reaction mechanism and its validation

5.3.1 Reaction chemistry of aqueous amine blend of TETA+DMAE+CO_2 system

A series of chemical reactions existed when the CO_2 gas was dissolved in the aqueous amine blend of TETA+DMAE. These reactions mainly involve the zwitterion mechanism, ter-molecular reaction mechanism, and base-catalyzed hydration mechanism. But, most of the researchers accepted the zwitterion mechanism for the aqueous alkanolamine solvents [1,31,33]. This mechanism was initially discovered by Caplow [61], and further investigation was carried out by Danckwerts [62]. In this mechanism, the earliest amine molecule in alkanolamine solvent (i.e., primary and secondary amine) reacts with the CO_2

gas, leading to zwitterion formation. This zwitterion species deprotonated with the second amine molecule and formed a carbamate complex. It was found that tertiary amines do not directly react with the CO_2 but act as a base catalyst that promotes CO_2 hydration [12,26], and Donaldson and Nguyen [63] gave this concept (Eq. 5.11 and 5.12). ^{13}C NMR spectroscopy was helpful in the determination and authentication of intermediate species present in the overall solution.

A series of chemical reactions are as follows:

Physical solubility:

$$CO_2\ (g) \overset{H_{CO_2}}{\longleftrightarrow} CO_2\ (aq.) \tag{5.6}$$

H_2O dissociation:

$$H_2O \overset{K1}{\leftrightarrow} H^+ + OH^- \tag{5.7}$$

Bicarbonate formation:

$$CO_2 + H_2O \overset{K2}{\leftrightarrow} HCO_3^- + H^+ \tag{5.8}$$

$$CO_2 + OH^- \overset{K3}{\leftrightarrow} HCO_3^- \tag{5.9}$$

Carbonate formation:

$$HCO_3^- \overset{K4}{\leftrightarrow} CO_3^{2-} + H^+ \tag{5.10}$$

DMAE intermediate reactions [5,21-22**]:**

$$DMAE + H^+ \overset{K5}{\leftrightarrow} DMAEH^+ \text{ (Protonated DMAE)} \tag{5.11}$$

$$CO_2 + DMAE + H_2O \overset{K6}{\leftrightarrow} DMAEH^+ + HCO_3^- \tag{5.12}$$

TETA intermediate reactions [31**]:**

$$TETA + CO_2 \overset{K7}{\leftrightarrow} TETA^+CO_2^- \tag{5.13}$$

$$TETA + TETA^{+}CO_2^{-} \overset{K8}{\leftrightarrow} TETAH^{+} + TETACO_2^{-} \quad (5.14)$$

$$TETACO_2^{-} + H_2O \overset{K9}{\leftrightarrow} HCO_3^{-} + TETA \quad (5.15)$$

$$TETA + CO_2 + H_2O \overset{K10}{\longleftrightarrow} HCO_3^{-} + TETAH^{+} \quad (5.16)$$

Overall reaction:

$$2TETA + 3DMAE + 4CO_2 + 4H_2O \overset{K11}{\longleftrightarrow} 3HCO_3^{-} + CO_3^{2-} + 2TETAH^{+} + 3DMAEH^{+} \quad (5.17)$$

H_{CO2}, K1-K11, and 5.6 to 5.17 represent the henry's constant, chemical reactions equilibrium constant, and reaction labels, respectively.

5.3.2 Nuclear magnetic resonance (NMR) spectroscopy

NMR analysis detected chemical species in the fresh and CO_2-loaded amine solvent. 0.6 ml of each amine solution was characterized by the ^{13}C NMR technique (Bruker Biospin international, Germany; Model no.: AVH D 500 AVANCE III HD 500MHz) at room temperature. It is the best analytical method [64] for determining carbon species in the aqueous amine blend solution [65-66]. It was operated at a frequency of 125.813 MHz, and its complete description was found in most of the literature [38-40,64]. $CDCl_3$ was used as an internal reference, and for enough signals, 0.3 ml of D_2O as deuterium lock was introduced in the amine blend samples. Different parameters used in the ^{13}C NMR experiments were the number of scans = 256, spectral width = 29761.904 Hz, acquisition time = 1.101 s, spectral frequency = 125.8131145 MHz, and time delay = 2 s.

5.4 Results and discussion

5.4.1 Validation of the experimental setup

To validate the experimental setup, 30 wt% MEA was used for the CO_2 absorption, operating at 313.15 K temperature and 8.09 kPa, 12.80 kPa, and 19.12 kPa CO_2 partial pressure. At this operating condition, the equilibrium CO_2 loading was found to be 0.532,

0.598, and 0.527 (mol CO_2/mol amine), respectively, which was comparable with the results so obtained in the literature [65-67]. The percentage average absolute relative deviation (% AARD) for equilibrium CO_2 loading was found to be 3.23 %. Table B15 of Appendix – B shows the experimental and literature data analyses that resembled each other in the acceptable % AARD. It means that the experimental setup was adequate for measuring equilibrium CO_2 loading for this current aqueous amine blend of TETA+DMAE.

5.4.2 Equilibrium CO_2 loading of the aqueous amine blend

In this work, the equilibrium CO_2 loading was estimated with the help of the aqueous amine blend of TETA+DMAE, operated in the semi-batch mode. There were four variables involved in the entire system, i.e., temperature (T), mole fraction of TETA (m_{TETA}), partial pressure of CO_2 (P_{CO2}), and solution concentration (C). The various sets of experiments were obtained using the Design-Expert software of trial version 8.0.6. A few separate experimental runs were also conducted, and the same is shown in Table 5.2.

Table 5.2 Experimental equilibrium CO_2 loading (α_{exp}) and calculated equilibrium CO_2 loading (α_{cal}) data of aqueous TETA+DMAE amine blend at different operating conditions such as CO_2 partial pressure (P_{CO2}, in kPa), mole fraction of TETA in the amine blend ($\mathbf{m_{TETA}}$), total amine blend concentration (C, in mol/L), and temperature (T, in K) at atmospheric pressure[a].

Run	Operating Parameters				α_{exp}	α_{cal}	ARD %
	T (K)	P_{CO2} (kPa)	m_{TETA}	C (mol/L)	(mol co_2/ mol amine)	(mol co_2/ mol amine)	
1.	315.65	17.73	0.05	1	0.6844	0.6910	0.964
2.	315.65	17.73	0.05	1.5	0.6538	0.6263	4.206
3.	298.15	17.73	0.13	1	0.8712	0.8839	1.457
4.	306.90	17.73	0.13	1	0.8532	0.8335	2.308
5.	315.65	17.73	0.13	1	0.8015	0.7807	2.595
6.	324.40	17.73	0.13	1	0.7322	0.7255	0.915
7.	333.15	17.73	0.13	1	0.6211	0.6680	7.551
8.	315.65	17.73	0.13	1.5	0.7258	0.7159	1.364
9.	315.65	17.73	0.20	1	0.9022	0.8695	3.624
10.	315.65	17.73	0.20	1.5	0.7950	0.8048	1.232
11.	315.65	17.73	0.05	2	0.6260	0.5738	8.338
12.	315.65	17.73	0.05	2.5	0.6100	0.5337	12.508
13.	315.65	10.13	0.13	2	0.5803	0.5894	1.568
14.	298.15	17.73	0.13	2	0.7027	0.7667	9.107

15.	306.90	17.73	0.13	2	0.6932	0.7163	3.332
16.	315.65	17.73	0.13	2	0.6830	0.6635	2.855
17.	324.40	17.73	0.13	2	0.5985	0.6083	1.637
18.	333.15	17.73	0.13	2	0.5078	0.5508	8.467
19.	315.65	25.33	0.13	2	0.6899	0.7114	3.116
20.	315.65	17.73	0.13	2.5	0.6655	0.6234	6.326
21.	315.65	17.73	0.20	2	0.7300	0.7523	3.054
22.	315.65	17.73	0.20	2.5	0.7200	0.7122	1.083
23.	315.65	17.73	0.05	3	0.6000	0.5059	15.683
24.	315.65	10.13	0.13	3	0.5432	0.5215	3.994
25.	298.15	17.73	0.13	3	0.6050	0.6988	15.504
26.	306.90	17.73	0.13	3	0.5885	0.6484	10.178
27.	315.65	17.73	0.13	3	0.6530	0.5955	8.805
28.	324.40	17.73	0.13	3	0.4900	0.5404	10.285
29.	333.15	17.73	0.13	3	0.4200	0.4828	14.952
30.	315.65	25.33	0.13	3	0.6700	0.6435	3.955
31.	315.65	17.73	0.20	3	0.7100	0.6844	3.605
						AARD % =	**5.631**

[a]Standard uncertainties u are u(T) = 1 K, u(P_{CO2}) = 0.05 kPa, u(m_{TETA}) = 0.001, u(C) = 0.01 mol/L and u(α) = 0.01 mol CO_2/ mol amine.

The experiments were carried out at atmospheric pressure, T = 298.15–333.15 K, m_{TETA} = 0.05–0.20, C = 1–3 mol/L, and P_{CO2} = 10.13–25.33 kPa. The percentage average absolute relative deviation (% AARD) of the separate experimental runs (except the RSM run sheet) was found to be 5.631 %.

5.4.2.1 Effect of mole fraction of activator (TETA) in the aqueous amine blend (TETA+DMAE) on equilibrium CO_2 loading

Most of the literature revealed that primary/secondary amines provide the equilibrium CO_2 loading up to 0.5 mol CO_2/mol amine, while tertiary amine can get up to 1 mol CO_2/mol amine [11]. Therefore, the aqueous amine blend of TETA+DMAE enhanced the reaction kinetics, possesses more absorption capacity and less regeneration energy. A few separate experiments were conducted to obtain the relationship between the equilibrium CO_2 loading and the effect of increasing the mole fraction of TETA in the amine blend. 0.05, 0.13, and 0.20 mole fraction of TETA were taken in the aqueous amine blend of TETA+DMAE. The total solution concentration was kept constant at 1 mol/L, 2 mol/L, and 3 mol/L. The whole experiments were performed at a constant temperature of 315.65 K and constant CO_2 partial pressure of 17.73 kPa. The linear relationship between the mole fraction of TETA and equilibrium CO_2 loading was obtained for each constant solution concentration. Figure 5.1 (a) indicated that increasing the mole fraction of the activator (TETA) from 0.05 to 0.20 also increased the equilibrium CO_2 loading of the aqueous amine blend of TETA+DMAE. The maximum equilibrium CO_2 loading was achieved at 0.20 mole fraction of TETA. Similar trends were also found for each constant solution concentration (i.e., 1 mol/L, 2 mol/L, and 3 mol/L).

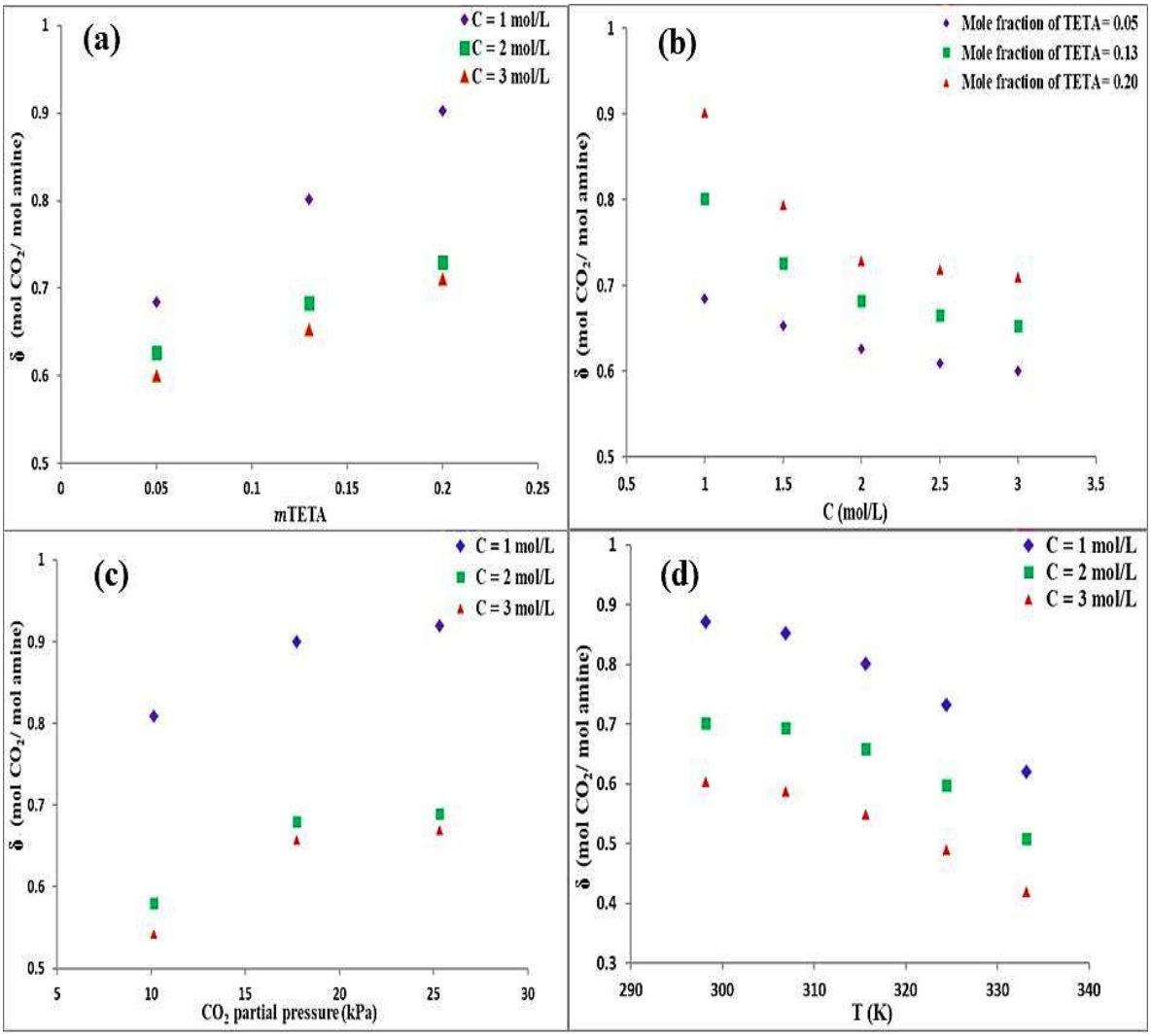

Figure 5.1 (a) Effect of mole fraction of TETA (m_{TETA}) on equilibrium CO_2 loading (α) at constant P_{CO2} = 17.73 kPa, T = 315.65 K, and at different C = 1, 2, and 3 mol/L (b) Effect of total solution concentration (C) on equilibrium CO_2 loading (α) at constant P_{CO2}= 17.73 kPa, T = 315.65 K, and at different m_{TETA} = 0.05, 0.13, and 0.2 (c) Effect of CO_2 partial pressure (P_{CO2}) on equilibrium CO_2 loading (α) at constant T = 315.65 K, m_{TETA} = 0.13, and at different C = 1, 2, and 3 mol/L (d) Effect of temperature (T) on equilibrium CO_2 loading (α) at constant P_{CO2}= 17.73 kPa, m_{TETA} = 0.13 and at different C = 1, 2, and 3 mol/L.

Therefore, increasing the mole fraction of TETA (polyamine) also increased the equilibrium CO_2 loading but simultaneously increased the heat of absorption. Further increasing the mole fraction of TETA could impart a high overall heat of absorption of the aqueous amine blend (TETA+DMAE). So, from most of the literature, the range of the mole fraction of TETA was limited from 0.05 to 0.20, and the same was also chosen for this work [8-9,10-11,13].

5.4.2.2 Effect of total concentration of aqueous amine blend of TETA+DMAE on equilibrium CO_2 loading

The role of overall aqueous amine blend solution concentration on equilibrium CO_2 loading is shown in Figure 5.1 (b). It was found that equilibrium CO_2 loading decreased on increasing the solution concentration from 1 to 3 mol/L for every fixed value of mole fraction of TETA, ranging from 0.05 to 0.20. The CO_2 partial pressure (P_{CO2}) and temperature (T) of the entire system were kept constant at 17.73 kPa and 315.65 K, respectively. As the mole fraction of TETA increased from 0.05 to 0.20 in the aqueous amine blend, then equilibrium CO_2 loading also increased substantially. The increase in solution concentration hindered the conversion of carbamate into bicarbonate, which ultimately reduced the equilibrium CO_2 loading [8-9,11,13]. According to Le Chatelier's principle, the concentration of mixed amine increases, the number of reactable amine molecules increases, but at the same time, the ratio of amine to carbon dioxide increases, this will lead to a lower equilibrium CO_2 loading. This analysis provided the best operating condition in terms of equilibrium CO_2 loading, and it was maximum for 0.20 mole fraction of TETA at 1 mol/L of solution concentration.

5.4.2.3 Effect of CO_2 partial pressure on equilibrium CO_2 loading

CO_2 partial pressure plays a significant role in determining the equilibrium CO_2 loading (α) in the gas-liquid system. The experiments were conducted for the three sets of constant solution concentration, i.e., 1 mol/L, 2 mol/L, and 3 mol/L, and CO_2 partial pressure (P_{CO2}) varied from 10.13–25.33 kPa. The temperature (T) and mole fraction of TETA (m_{TETA}) were kept constant at 315.65 K and 0.13, respectively. The relationship between the 'P_{CO2}' vs. 'α' (mol CO_2/mol amine) was estimated in the above specified operating conditions. Figure 5.1 (c) concluded that increasing the CO_2 partial pressure also increases the equilibrium CO_2 loading [11]. It was happened due to the transfer of additional CO_2 gas molecules to the gas-liquid interface because of increasing driving force. The concept of Henry's law was applicable in the case of the physical solubility of a gas in the liquid. Therefore, with increasing CO_2 partial pressure in the gas stream, more CO_2 gas was dissolved in the liquid phase as governed by Henry's law, forming a large amount of carbamate, carbonate, and bicarbonate. The experimental results showed that equilibrium CO_2 loading increased significantly up to 17.73 kPa, but moderate growth of equilibrium CO_2 loading was seen after this.

5.4.2.4 Effect of temperature on equilibrium CO_2 loading for the aqueous amine blend of TETA+DMAE

In order to analyze the effect of temperature on equilibrium CO_2 loading, the experiments were conducted in the temperature range of 298.15–333.15 K. CO_2 Partial pressure (P_{CO2}) and mole fraction of TETA (m_{TETA}) remained constant at 17.73 kPa and 0.13, respectively. The correlation between the temperature (T) and equilibrium CO_2 loading (α) was obtained for the different sets of constant solution concentrations (C) at 1

mol/L, 2 mol/L, and 3 mol/L. Figure 5.1 (d) showed a relationship between 'T' vs. 'α', and it was found that the equilibrium CO_2 loading was decreasing for all constant solution concentration on increasing the temperature. As the temperature increases, the gas-liquid equilibrium shifts in the reverse direction [8,11]. Also, at a high temperature, desorption of CO_2 gas takes place, which ultimately retards the equilibrium CO_2 loading in the aqueous amine blend. As a result, the absorption process is unfavorable at high temperatures, as stated by Le Chatelier's principle.

5.4.3 Development of an empirical model for the TETA+DMAE aqueous amine blend

An empirical model was developed to predict the equilibrium CO_2 loading in the aqueous amine blend of TETA+DMAE. The value of equilibrium CO_2 loading obtained by this model (α_{cal}) would be helpful in authenticating the experimental results. Four parameters, temperature (T), mole fraction of TETA (m_{TETA}), partial pressure of CO_2 (P_{CO2}), and solution concentration (C), were used to develop such a model. This model was valid for T = 298.15–333.15 K, m_{TETA} = 0.05–0.20, P_{CO2} = 10.13–25.33 kPa, and C = 1–3 mol/L. The equation of the empirical model based on the above parameters is expressed as:

$$\alpha_{cal} = x_1 + x_2 T + x_3 T^2 + x_4 P_{CO2} + x_5 P_{CO2}^2 + x_6 m_{TETA} + x_7 m_{TETA}^2 + x_8 C + x_9 C^2 \quad (5.18)$$

Where, α_{cal} is the equilibrium CO_2 loading calculated by the empirical model (mol CO_2/mol amine), x_1–x_9 are the unknown coefficients of the model, T is the temperature (in kelvin), P_{CO2} is the CO_2 partial pressure (in kPa), m_{TETA} is the mole fraction of TETA, and C is the solution concentration (in mol/L).

To obtain the value of α_{cal}, it was essential to achieve the values of unknown coefficients of the model equation. From Table 5.2, utilizing the experimental set of data under specified operating conditions and Microsoft Excel solver software benefitted to provide the values of unknown coefficients, and their values are listed in Table B16 of Appendix – B. Now, using the unknown values and different experimental operating conditions, α_{cal} values for each data set have been calculated and finally reported. Percentage absolute relative deviation (% ARD) and percentage average absolute relative deviation (% AARD) for the experimental (α_{exp}) and calculated (α_{cal}) equilibrium CO_2 loading was estimated by using Eq. 5.19 and Eq. 5.20.

$$\% \text{ ARD } = \frac{|\alpha_{exp} - \alpha_{cal}|}{\alpha_{exp}} \times 100 \quad (5.19)$$

$$\% \text{ AARD } = \frac{1}{N} \times \sum_{i=1}^{N} \frac{|\alpha_{exp} - \alpha_{cal}|}{\alpha_{exp}} \times 100 \quad (5.20)$$

Where N is the no. of the experimental set of data points, α_{exp} is the experimentally calculated equilibrium CO_2 loading, α_{cal} is the equilibrium CO_2 loading estimated by the developed empirical model. The relationship between the equilibrium CO_2 loading obtained by the actual experiments (α_{exp}) and model calculated empirical data (α_{cal}) is depicted in Figure A10 of Appendix – A. Under specified operating conditions, a reliable AARD of 5.631 % was obtained, which was in good agreement of the equilibrium CO_2 loading for the empirical model's value and experimentally calculated values. Therefore, the developed model equation for this experimental work is authenticated, correct, and highly acceptable.

5.4.4 CO_2 desorption analysis

Cyclic capacity and cyclic equilibrium CO_2 loading are essential aspects for selecting the perfect absorbent for CO_2 capture from the industrial point of view. In order to estimate

the cyclic capacity of the aqueous amine blend of TETA+DMAE, desorption experiments were performed. The run sheet generated by the RSM software provided the idea on which the desorption study had to be conducted. All desorption experiments for the CO_2 saturated samples were performed at the constant temperature of 393.15 K and constant CO_2 partial pressure of 17.73 kPa. From Table 5.3, eight run samples from this RSM-generated table were found to operate at a constant pressure of 17.73 kPa and the corresponding temperature of 315.65 K. In all such run samples, one of the runs had a concentration of 1 mol/L, six runs had a 2 mol/L concentration and the last run had a 3 mol/L concentration of the entire solution. The CO_2 loading after desorption experiment was found to be 0.1255, 0.1545, and 0.2704, corresponding to 1 mol/L, 2 mol/L, and 3 mol/L of the solution concentration, respectively. The average value of all the six run samples was reported for the 2 mol/L solution concentration. Figure 5.2 depicts the cyclic capacity and cyclic equilibrium CO_2 loading of 30 wt% (i.e., 5 mol/L) of MEA solution and aqueous amine blend of TETA+DMAE from 1 to 3 mol/L of the solution concentration. The aqueous amine blend of 3 mol/L of TETA+DMAE showed 55.03 % higher cyclic loading capacity than 30 wt% of MEA. This aqueous amine blend solution would necessitate a smaller equipment size and a lower absorption circulation rate in a CO_2 capture system plant.

Table 5.3 Experimental runs generated by the response surface methodology (RSM) for the aqueous amine blend of TETA+DMAE and the equilibrium CO_2 loading (Y) as a final response at different operating conditions (T, P_{CO2}, m_{TETA}, C, and atmospheric pressure[a]).

Run	Operating Parameters				Response (Y)	α_{cal}	ARD %
	T (K)	P_{CO2} (kPa)	m_{TETA}	C (mol/L)	(mol co_2/ mol amine)	(mol co_2/ mol amine)	
1.	324.40	13.93	0.09	2.50	0.4825	0.4799	0.538
2.	315.65	17.73	0.13	2.00	0.6585	0.6587	0.030
3.	306.90	21.53	0.16	2.50	0.6899	0.7056	2.275
4.	333.15	17.73	0.13	2.00	0.5078	0.5483	7.975
5.	306.90	13.93	0.16	2.50	0.6100	0.6533	7.098
6.	306.90	21.53	0.16	1.50	0.8120	0.8363	2.992
7.	306.90	21.53	0.09	2.50	0.6561	0.6377	2.804
8.	315.65	17.73	0.13	2.00	0.7027	0.6587	6.261
9.	315.65	17.73	0.13	1.00	0.9200	0.8531	7.271
10.	315.65	10.13	0.13	2.00	0.5803	0.5600	3.498
11.	324.40	21.53	0.09	2.50	0.5909	0.5322	9.933
12.	306.90	13.93	0.09	2.50	0.5992	0.5854	2.303
13.	324.40	13.93	0.16	1.50	0.6561	0.6784	3.398

14.	315.65	17.73	0.13	3.00	0.5500	0.5917	7.047
15.	324.40	13.93	0.09	1.50	0.6268	0.6105	2.600
16.	315.65	17.73	0.05	2.00	0.6264	0.5863	6.401
17.	324.40	13.93	0.16	2.50	0.5099	0.5477	7.413
18.	315.65	17.73	0.20	2.00	0.7109	0.7317	2.925
19.	324.40	21.53	0.16	1.50	0.6281	0.7307	16.335
20.	315.65	17.73	0.13	2.00	0.6830	0.6587	3.557
21.	306.90	21.53	0.09	1.50	0.7832	0.7684	1.889
22.	298.15	17.73	0.13	2.00	0.6852	0.7594	10.828
23.	315.65	17.73	0.13	2.00	0.6920	0.6587	4.812
24.	315.65	17.73	0.13	2.00	0.6800	0.6587	3.132
25.	315.65	25.33	0.13	2.00	0.6899	0.6646	3.667
26.	324.40	21.53	0.16	2.50	0.6432	0.6000	6.716
27.	315.65	17.73	0.13	2.00	0.6732	0.6587	1.450
28.	324.40	21.53	0.09	1.50	0.6645	0.6629	0.240
29.	306.90	13.93	0.09	1.50	0.7248	0.7161	1.200
30.	306.90	13.93	0.16	1.50	0.7645	0.7840	2.550
						AARD % =	**4.638**

[a]Standard uncertainties u are u(T) = 1 K, u(P_{CO2}) = 0.05 kPa, u(m_{TETA}) = 0.001, u(C) = 0.01 mol/L and u(Y) = 0.01 mol CO_2/ mol amine.

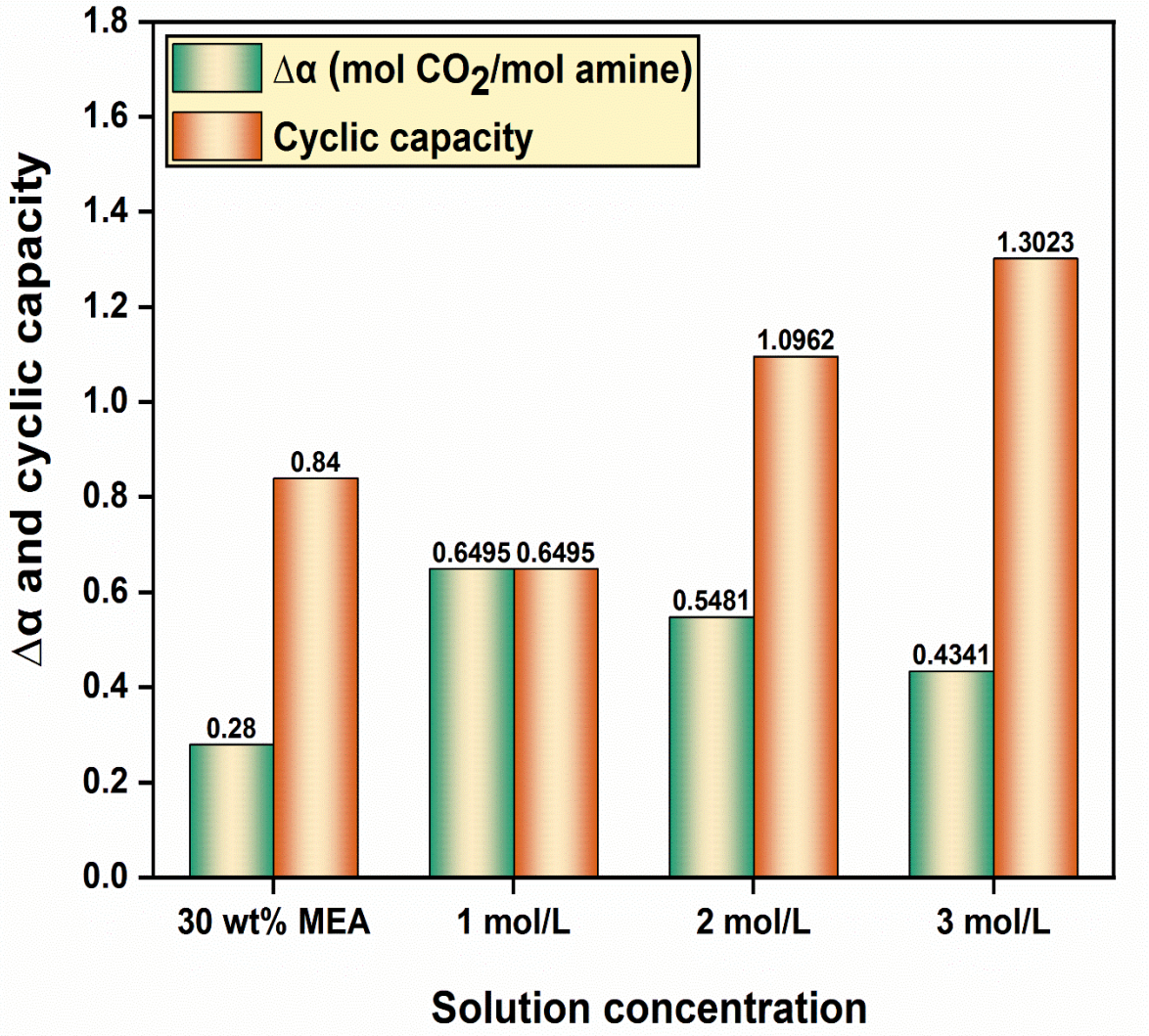

Figure 5.2 Cyclic equilibrium CO_2 loading and cyclic capacity of 30 wt% MEA solution and aqueous amine blend of TETA+DMAE with m_{TETA} = 0.13 at C = 1 mol/L, 2 mol/L and 3 mol/L.

5.4.5 Heat of CO_2 absorption

The heat of absorption is the heat liberated during CO_2 absorption that takes place in the aqueous amine blend of TETA+DMAE. The higher value of ΔH_{abs} indicates that there is an excessive requirement of regeneration's heat and vice-versa. ΔH_{abs} can be experimentally estimated with the help of a calorimeter instrument [59] and theoretically by using the Gibbs-Helmholtz equation [1,45,58-60]. In this research work, ΔH_{abs} was calculated by using the Gibbs-Helmholtz equation. The RSM software generated a run sheet with different experimental runs, as shown in Table 5.3. After performing the actual experiments on the lab scale, it was found that at different temperatures (T) and CO_2 partial pressures (P_{CO2}), some of the equilibrium CO_2 loading was found to be constant. Such run points were taken into consideration for the estimation of ΔH_{abs}. Three data points of P_{CO2} and $\frac{1}{T}$ were chosen that have nearly the same equilibrium CO_2 loading of 0.61 and 0.68 (mol of CO_2/mol amine). A plot was drawn in between $d\ln(P_{CO2})$ and $d(\frac{1}{T})$ as shown in Figure 5.3, and their corresponding slope of the line was found to be -8073.3 and -8076.7. The product of the average value of the above slopes and the universal gas constant (R = 8.314 J/(mol.K)) provided the value of ΔH_{abs}. The heat of CO_2 absorption of the aqueous amine blend of TETA+DMAE was found to be -67.135 kJ/mol. In this case, the ΔH_{abs} value is negative, indicating that the reaction system is exothermic in nature. This system's ΔH_{abs} value revealed that it is lower than tertiary amine (MDEA = -54.6 kJ/mol) [25], but greater than the industrial benchmark primary amine (MEA = -85.13 kJ/mol) [15].

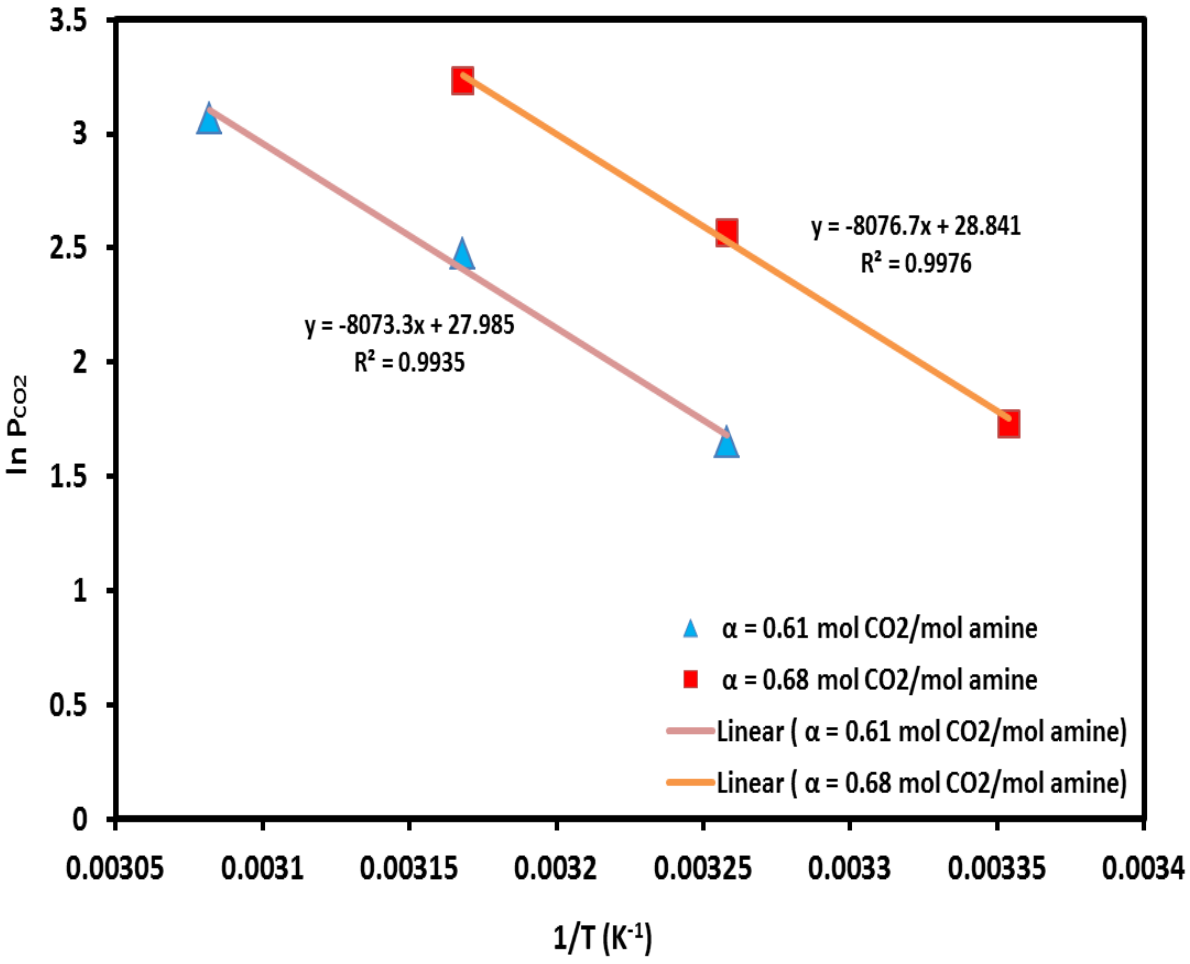

Figure 5.3 Plot of ln (P_{CO2}) vs. ($\frac{1}{T}$) at different equilibrium CO_2 loading for estimating heat of absorption (ΔH_{abs}) for the aqueous amine blend of TETA+DMAE.

5.4.6 ^{13}C NMR spectral analysis

The aqueous amine blend of TETA+DMAE solution was prepared on the lab scale of different chemical compositions. The analysis of the chemical species available in the solution system was done with the help of ^{13}C NMR spectral analysis [23,26]. NMR study was performed on two types of samples: pure amine blend solution (without CO_2 loading) and CO_2-loaded amine blend solution. Any CO_2-loaded amine sample under any operating conditions could be chosen for the analyses, but the sample with the highest equilibrium CO_2 loading was selected for this work. In the analyses, the pure amine blend solution showed chemical shifts ranging from 40.08 to 73.43 ppm. Zheng et al. [36] revealed that the NMR spectrum of TETA peaks is available between 35–50 ppm. Figure 5.4 (a) shows the TETA and DMAE species in the pure amine blend solution. The peaks from 40.08–49.79 ppm showed the abundance of the TETA species, whereas peaks in the range of 60.67–61.96 ppm were responsible for the DMAE in the pure amine blend solution. Figure 5.4 (b) represents the various peaks of the CO_2-loaded amine blend solution. It was found to have a chemical shift of 40.70–49.84 ppm for $TETAH^+$ and 60.70–61.47 ppm for $DMAEH^+$. In reaction with CO_2, the peaks at 164.13 ppm and 166.47 ppm were formed in the carbonyl region (C = O) due to bicarbonate and carbonate species formation. In most of the literature, it was found that the peaks of bicarbonate/carbonates lay in the range of 160–168 ppm [35,37-38,40]. Table B17 of Appendix – B represents the chemical species available in the amine blend before and after CO_2 loading.

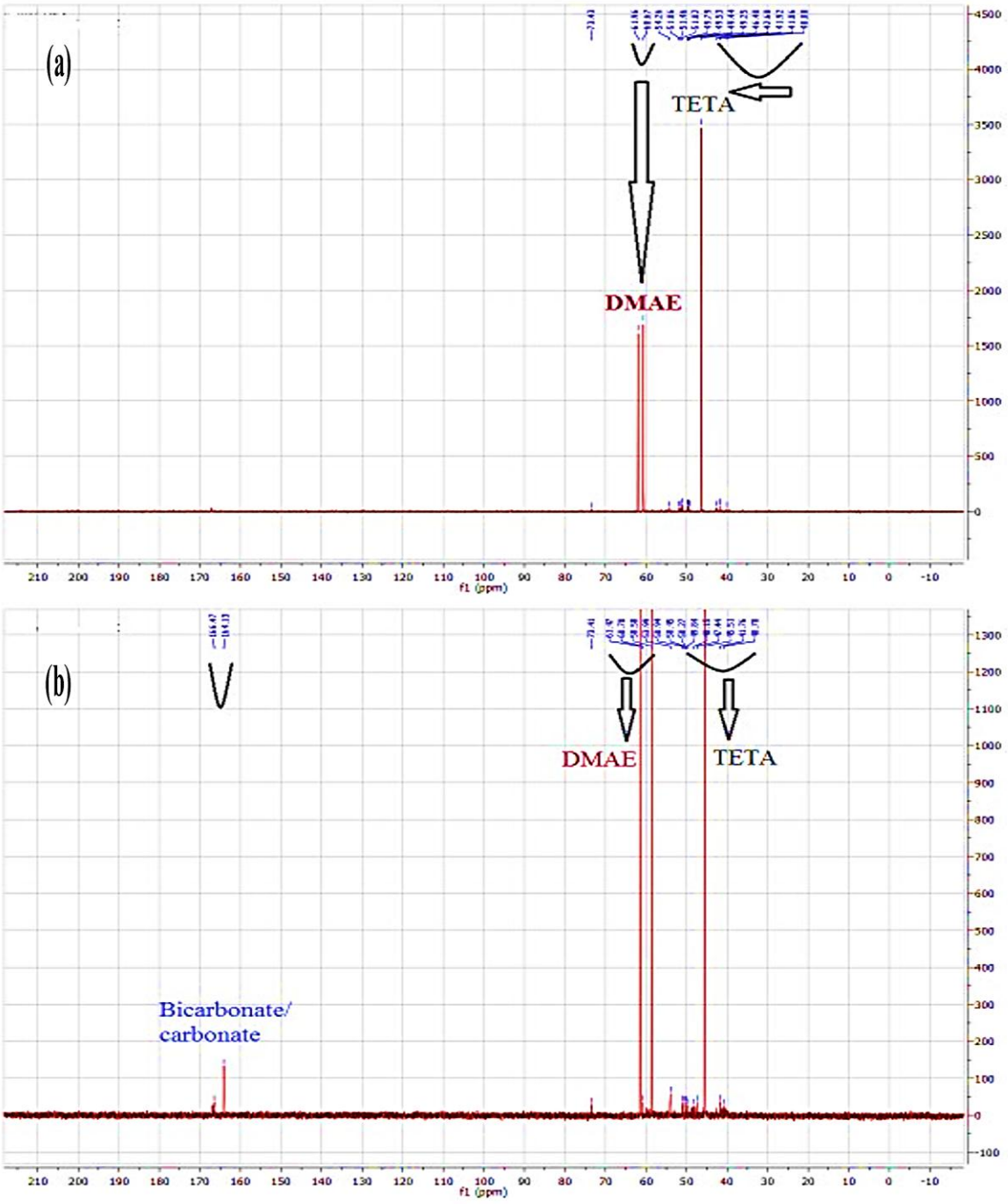

Figure 5.4 ^{13}C NMR analyses of aqueous amine blend of TETA+DMAE (a) before CO_2 loading (b) after CO_2 loading.

5.4.7 Response surface methodology (RSM) analysis

Response surface methodology (RSM) is a multivariable statistical approach for optimizing almost any type of process [47-49]. The objective function in this work is the equilibrium CO_2 loading, which is affected by four variables: temperature (T), mole fraction of TETA (m_{TETA}), solution concentration (C), and CO_2 partial pressure (P_{CO2}). These four variables are input variables, whereas the equilibrium CO_2 loading as the final response (Y) was referred to as an output variable. A generalized quadratic model can be defined as:

$$Y = \varphi 0 + \sum_{i=1}^{k} \varphi i\, Xi + \sum_{i=1}^{k} \varphi ii X_i^2 + \sum \sum_{i<j} \varphi ij\, Xi\, Xj \quad (5.21)$$

where Y represents the final response, φ_0 represents the constant coefficient, φi represents the linear constant coefficient, φii represents the quadratic constant coefficient, and φij represents the interaction coefficient. Furthermore, Xi and Xj are the independent encoded variables used throughout the experiment. Eq. 5.21 predicts the response behavior in the experimental set of data points as a function of independent variables. The detailed description of RSM analysis has already been discussed in Section 3.4.11 of Chapter 3.

5.4.7.1 Development and analysis of equilibrium CO_2 loading as a final response using response surface methodology

In this present work, maximizing the equilibrium CO_2 loading of the aqueous amine blend of TETA+DMAE was the prime objective. Design expert software of version 8.0.6 benefitted from providing the entire run sheet at various operating conditions. Initially, it was mandatory to input the values of the independent variables i.e. T = 298.15–333.15 K, m_{TETA} = 0.05–0.20, C = 1–3 mol/L, and P_{CO2} = 10.13–25.33 kPa. These independent variables are known as factors in this software, so temperature (T), mole fraction of TETA

(m_{TETA}), solution concentration (C), and partial pressure of CO_2 (P_{CO2}) were assigned as factors A, B, C, and D, respectively. For this present work, the central composite design (CCD) method with the quadratic model was adopted to maximize the final response. RSM software generated 30 such run samples, in which 24 runs were defined as non-central points, whereas 6 runs were identified as central points. Table 5.3 shows the experimental runs created by the RSM software under different operating conditions (T, P_{CO2}, m_{TETA} and C). Equilibrium CO_2 loading was estimated as a final response (Y) by carrying out the actual experiments on the lab scale under the specified operating conditions. The final response was also analyzed by the developed model (α_{cal}), and it was estimated using Eq. 5.18. The values of unknown coefficients in Eq. 5.18 were achieved using a Microsoft Excel solver, and their values are listed in Table B18 of Appendix – B. This experimental run sheet acquired a good AARD of 4.638 % and was in a highly acceptable zone. Table 5.4 displays all four independent variables and their corresponding coded levels, as shown in the design summary section of the RSM software.

Table 5.4 Experimental independent variables and their coded levels used for Central Composite design for the estimation of equilibrium CO_2 loading as a final response.

Independent variable	**Symbol**	**Coded Levels**				
		-α	**-1**	**0**	**+1**	**+ α**
Temperature	A	298.15	306.90	315.65	324.40	333.15
Mole fraction of TETA	B	0.05	0.09	0.13	0.16	0.20
Solution concentration	C	1	1.5	2	2.5	3
Partial pressure of CO_2	D	10.13	13.93	17.73	21.53	25.33

5.4.7.2 RSM generated model and its validation

It was critical to target the analysis of variance (ANOVA) results in order to judge the significance of the chosen quadratic model in CCD. The ANOVA provides different values for the sum of squares, degree of freedom (df), mean square value, F-value, and P-value. This analysis also provided the various interactions between the independent variables like AB, AC, AD, BC, BD, CD, A^2, B^2, C^2, and D^2. The values of all the factors in the ANOVA were helpful in determining whether the applied model is significant or not. Table 5.5 indicates the results of the ANOVA test in which the equilibrium CO_2 loading was referred to as the final response of the entire system. From Table 5.5, it was found that the model F-value was 16.75, which implied that the model was significant. Similarly, the values of 'Prob > F' must be less than 0.0500 for the model to be significant, and for this present situation, it was < 0.0001. If the values for A, B, C, D, A^2, and D^2 are greater than 0.1000, the model is insignificant; however, in our case, all such values were less than 0.0001. RSM software provided the values of all unknown coefficients of the independent variables. On putting all these values in Eq. 5.21, the final response in terms of equilibrium CO_2 loading was obtained as follows:

$$\text{Response (Y)} = 0.68 - 0.050A + 0.015B - 0.067C + 0.030D - 0.002531AB + 0.011AC + 0.0005438AD + 0.003931BC - 0.001794BD + 0.016CD - 0.022A^2 - 0.004264B^2 + 0.012C^2 - 0.013D^2 \quad (5.22)$$

Table 5.5 ANOVA analysis of quadratic model in CCD for the estimation of equilibrium CO_2.

Source	Sum of squares	df	Mean square	F value	p-value Prob > F	
Model	0.23	14	0.016	16.75	< 0.0001	Significant
A-Temperature	0.059	1	0.059	61.56	< 0.0001	
B-Mole fraction of TETA	5.242E-003	1	5.242E-003	5.45	0.0339	
C-Solution concentration	0.11	1	0.11	113.37	< 0.0001	
D-Partial pressure of CO_2	0.021	1	0.021	22.03	0.0003	
AB	1.025E-004	1	1.025E-004	0.11	0.7487	
AC	2.032E-003	1	2.032E-003	2.11	0.1669	
AD	4.731E-006	1	4.731E-006	4.915E-003	0.9450	
BC	2.473E-004	1	2.473E-004	0.26	0.6196	
BD	5.148E-005	1	5.148E-005	0.053	0.8202	
CD	4.320E-003	1	4.320E-003	4.49	0.0512	
A^2	0.014	1	0.014	14.17	0.0019	
B^2	4.986E-004	1	4.986E-004	0.52	0.4828	
C^2	4.166E-003	1	4.166E-003	4.33	0.0550	
D^2	4.390E-003	1	4.390E-003	4.56	0.0496	
Residual	0.014	15	9.625E-004			
Lack of Fit	0.013	10	1.328E-003	5.71	0.0341	Non-Significant
Pure Error	1.162E-003	5	2.324E-004			
Cor Total	0.24	29				

This ANOVA analysis provided the statistical parameters like standard deviation, mean, R-square value, adjusted R-square value, predicted R-square value, etc., and the same is shown in Table B19 of Appendix – B. The values of all such statistical parameters must be close to 1 to validate the model for the experimental task. In our case, the R-square value is 0.9399, the adjusted R-square value is 0.8838, and the predicted R-square value is 0.6746. Adequate precision measures the signal to the noise ratio, and if its ratio is greater than 4, then it is desirable; in our case, it is found to be 17.393, which indicates an adequate signal, so the model can be used to navigate the design space. The coefficient of variance (CV %) in this case was 4.70 %, suggesting that there was less standard deviation than the mean. The predicted R-square value was much closer to the adjusted R-square value, so it can be concluded these values validate the model. The relationship between the actual and the predicted equilibrium CO_2 loading is shown in Figure 5.5 (a). The values of the response of actual experiments were very much closer to the predicted value of the equilibrium CO_2 loading. This is clear evidence that the developed model successfully calculated equilibrium CO_2 loading. The normal plot of residual is shown in Figure 5.5 (b); it provides the correlation between the normal % probability and internally studentized residuals. The residuals were generally distributed along a straight line, indicating that the errors were distributed normally. Figure 5.5 (c) established a relationship between the internally studentized residuals vs. predicted values of the equilibrium CO_2 loading. The randomly distributed plot shows that the variance of the original observations is constant for all of the obtained responses [54,56]. Figure 5.5 (d) shows a relationship between internally studentized residuals and run numbers for the equilibrium CO_2 loading.

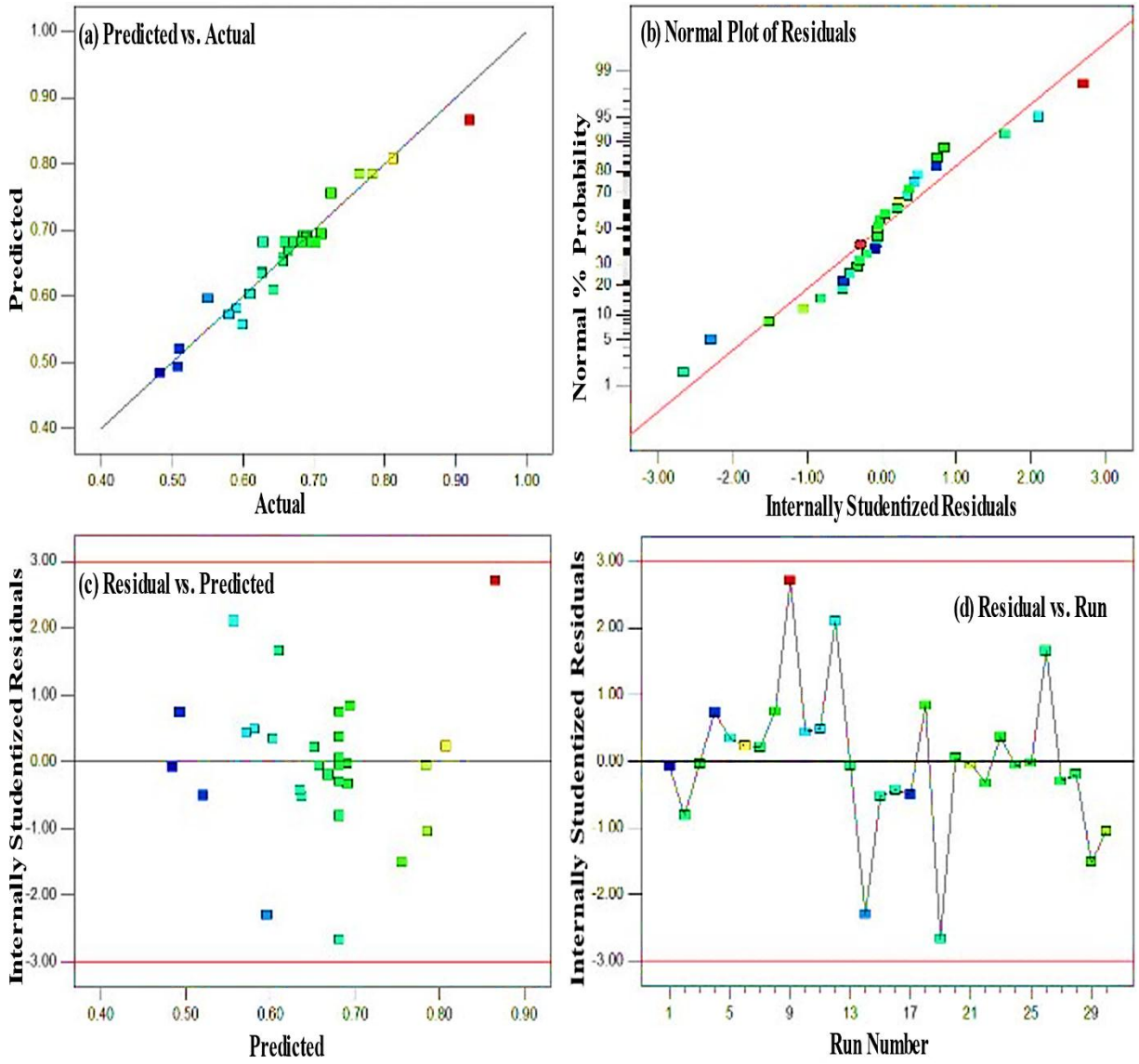

Figure 5.5 (a) The actual vs. predicted plot of equilibrium CO_2 loading as a final response (b) The plot of internally studentized residuals vs. normal percentage probability of equilibrium CO_2 loading (c) The predicted equilibrium CO_2 loading and internally studentized residuals plot (d) Internally studentized residuals versus the run number.

This plot demonstrated that no proper relationship existed between the observed outputs and the order of the experimental set of data points. RSM software itself created different runs corresponding to various independent variables (T, m_{TETA}, P_{CO2}, and C). Figure A11 (a), (b), (c), and (d) of Appendix – A was the representation of run points vs. equilibrium CO_2 loading at different operating conditions of temperature, mole fraction of TETA, solution concentration, and partial pressure of CO_2, respectively. After examining all of the parameters, it is clear that CCD passed all of the statistical tests.

5.4.7.3 Analysis of 3-D surfaces and contour graphs

3-D surfaces and contour graphs are general representations of the study's chosen model. It provided a clear picture of the effectiveness of independent variables and the final output response within the domain preferred for the complete analysis. Figure 5.6 (a) and (b) represent the 3-D curve and the contour plot, respectively, which correlate temperature (A) and mole fraction of TETA (B) with the equilibrium CO_2 loading as a final response. These figures themselves suggested that at low temperature and high mole fraction of TETA, the value of the final response would be maximum, and the same was also proved in the previous section. The 3-D curve and the contour plot in Figure 5.6 (c) and (d) represented the interaction between temperature (A), solution concentration (C), and final response. The 3-D curve and the contour plot concluded that the final response was highest at low temperature and low solution concentration. Figure 5.7 (a) and (b) depicted a 3-D curve and a contour plot, respectively, correlating temperature (A), partial pressure of CO_2 (D), and equilibrium CO_2 loading. According to this 3-D curve and contour plot, the final response was maximum at low temperature and high CO_2 partial pressure.

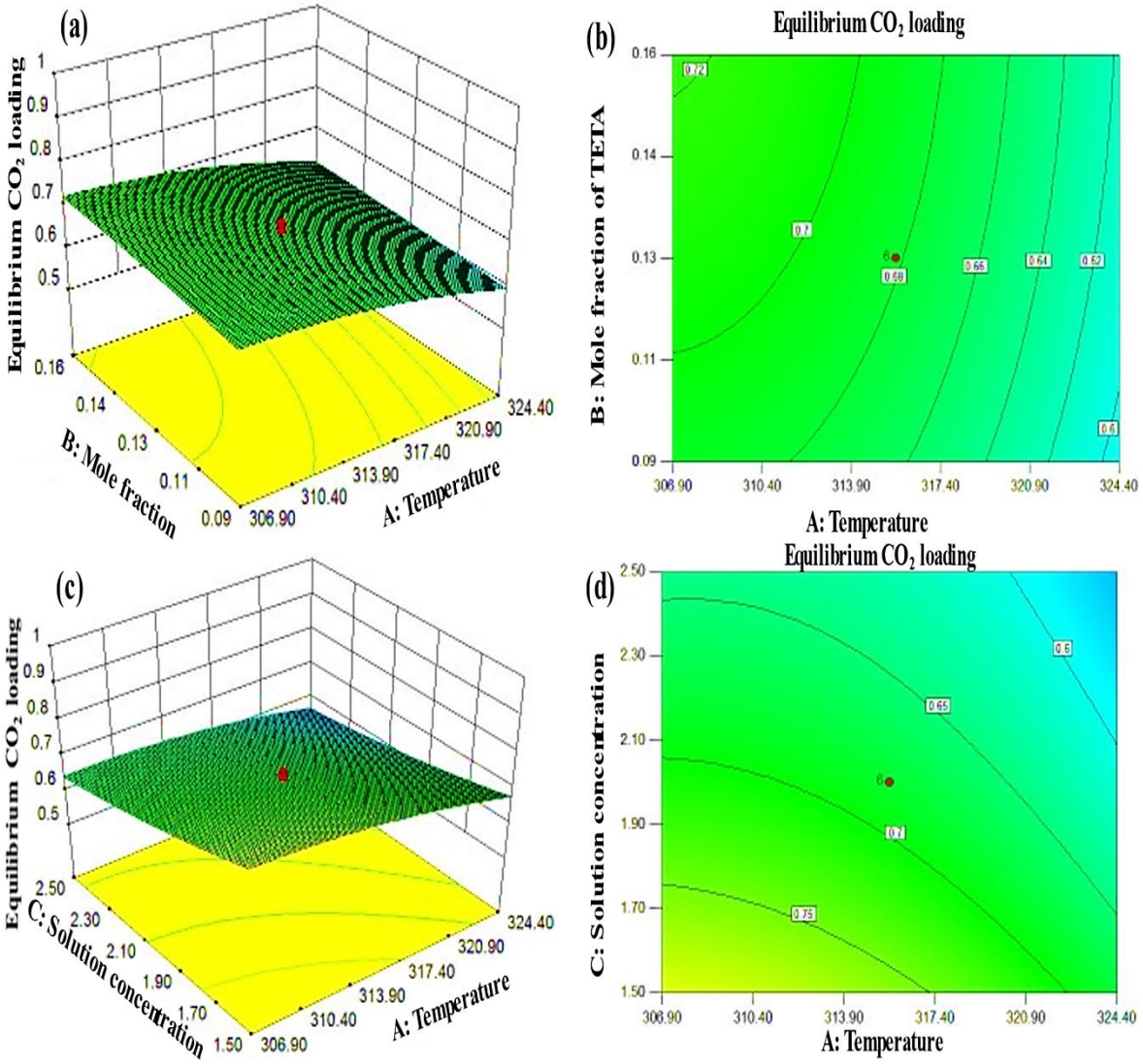

Figure 5.6 (a) 3-D surface representation of temperature (A), mole fraction of TETA (B), and equilibrium CO_2 loading (b) Contour plot showing the effect of temperature (A), mole fraction of TETA (B) on equilibrium CO_2 loading (c) 3-D surface representation of temperature (A), solution concentration (C), and equilibrium CO_2 loading (d) Contour plot showing the effect of temperature (A), solution concentration (C) on equilibrium CO_2 loading.

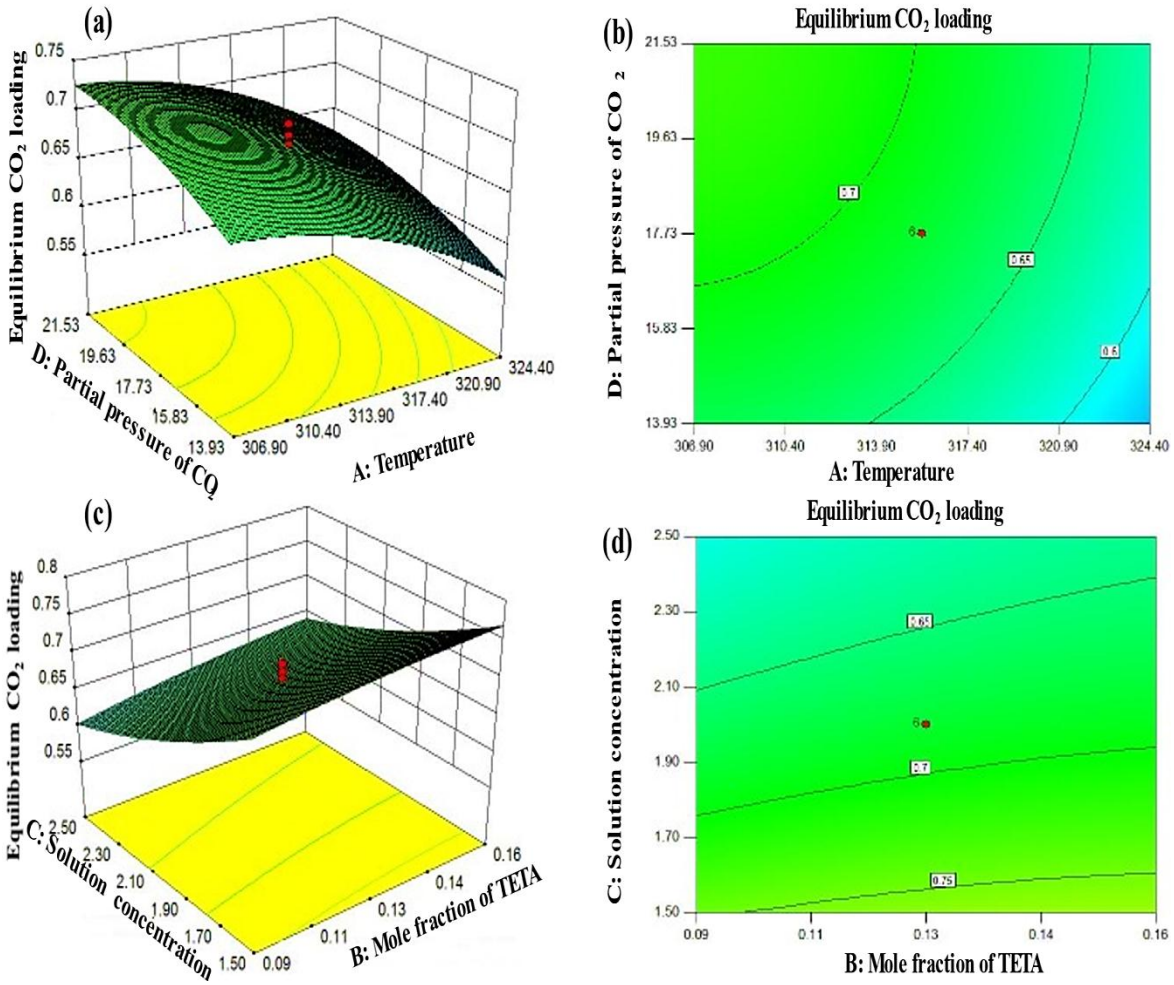

Figure 5.7 (a) 3-D surface representation of temperature (A), partial pressure of CO_2 (D), and equilibrium CO_2 loading (b) Contour plot showing the effect of temperature (A) and partial pressure of CO_2 (D) on equilibrium CO_2 loading (c) 3-D surface representation of mole fraction of TETA (B), solution concentration (C), equilibrium CO_2 loading (d) Contour plot showing the effect of mole fraction of TETA (B) and solution concentration (C) on equilibrium CO_2 loading.

Likewise, Figure 5.7 (c) and (d) represent the relationship between the independent factors of mole fraction of TETA (B) and solution concentration (C), corresponding to the equilibrium CO_2 loading as a final response. Finally, the above 3-D curve and contour plot showed that increasing the mole fraction of TETA increased equilibrium CO_2 loading while increasing solution concentration decreased equilibrium CO_2 loading. Therefore, the final response was maximum for the immense value of mole fraction of TETA and low value of solution concentration. Figure 5.8 (a) and (b) are the 3-D curve and contour plots, respectively, that correlated the presence of mole fraction of TETA (B) and the partial pressure of CO_2 (D) that was ultimately affecting the equilibrium CO_2 loading as a final response. It was found that the final response was maximum at a high value of mole fraction of TETA and partial pressure of CO_2. Finally, the relationship between the solution concentration (C) and partial pressure of CO_2 (D) with respect to equilibrium CO_2 loading as a final response is depicted in Figure 5.8 (c) and (d). The response in terms of equilibrium CO_2 loading increased with increased CO_2 partial pressure and a decrease in solution concentration. The reasons for all the above results have already been discussed in the previous sections.

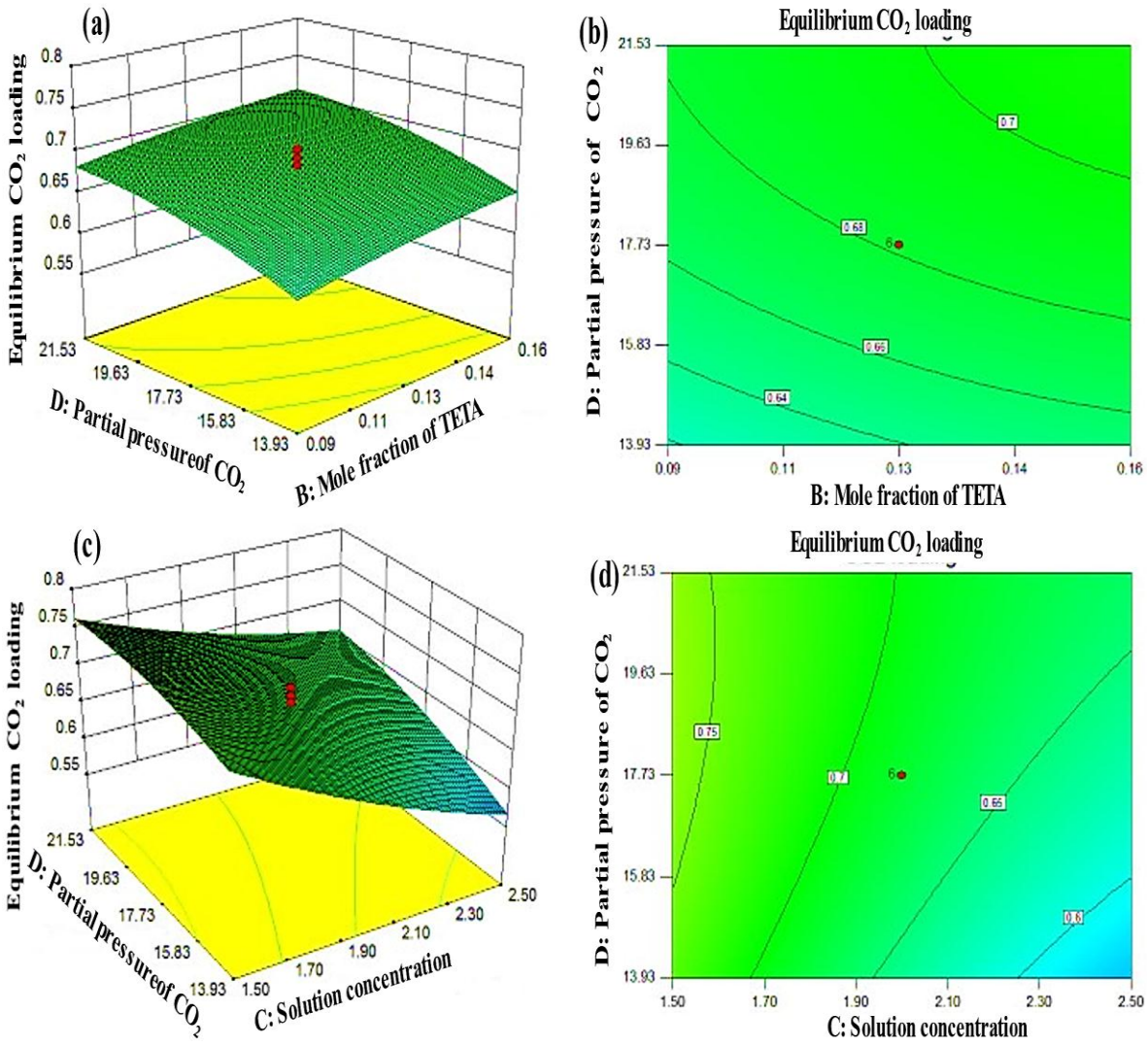

Figure 5.8 (a) 3-D surface representation of mole fraction of TETA (B), partial pressure of CO_2 (D), and equilibrium CO_2 loading (b) Contour plot showing the effect of mole fraction of TETA (B) and partial pressure of CO_2 (D) on equilibrium CO_2 loading (c) 3-D surface representation of solution concentration (C), partial pressure of CO_2 (D), and equilibrium CO_2 loading (d) Contour plot showing the effect of solution concentration (C) and partial pressure of CO_2 (D) on equilibrium CO_2 loading.

5.4.7.4 Prediction of the optimum value and its verification by the RSM software

The RSM software was used to optimize the equilibrium CO_2 loading as the final response, and it also provided the optimum values of the rest other factors involved in the entire system. Table B20 of Appendix – B depicts the desired goal, importance, lower and upper limits of all the input independent variables in relation to the final response. When such variables and responses were combined, they formed an overall desirability function that must be optimized. In the numerical optimization section of the RSM software, it was essential to set the goal for each response, and then further software calculated the optimal solutions. Figure A12 of Appendix – A shows the ramp solutions of the independent variables at which the optimum results were obtained. At temperature (T) = 304.36 K, mole fraction of TETA (m_{TETA}) = 0.14, solution concentration (C) = 1.0 and partial pressure of CO_2 (P_{CO2}) = 17.24 kPa the optimum equilibrium CO_2 loading as a final response was found to be 0.926207 mol CO_2/mol amine. The system's desirability is determined by the final response value's proximity to the ideal value, ranging from 0 to 1. For this work, the desirability of the final response was found to be 0.856, which is very close to one. It was critical to authenticate the optimal results provided by the RSM software. Therefore, two aqueous amine blend solutions of TETA+DMAE with solution concentration much closer (i.e., 0.9 mol/L and 1.1 mol/L) to the optimal range were prepared on the lab scale. The other operating conditions like T = 304.36 K, m_{TETA} = 0.14, and P_{CO2} = 17.24 kPa remained unaffected. The average value of the equilibrium CO_2 loading was 0.924825 mol CO_2/mol amine, which is less than 1 % of the predicted value. Therefore, the actual experimental results authenticate the predicted values. Table B21 of Appendix – B

indicates the optimization results of the predicted and actual experimental values. Hence, it is a verification test to compare the results between them.

5.5 Conclusions

This work studied the CO_2 gas absorption and its desorption behavior of the novel aqueous amine blend of TETA+DMAE. In the absorption section, the experiments were performed at temperature (T) = 298.15–333.15 K, mole fraction of TETA (m_{TETA}) = 0.05–0.20, solution concentration (C) = 1–3 mol/L and partial pressure of CO_2 = 10.13–25.33 kPa. The RSM software and some separate experimental runs were created the operational sets under these operating conditions. The effects of all of the aforementioned factors on the equilibrium CO_2 loading were assessed. After performing various experiments at the specified operating conditions, the optimum equilibrium CO_2 loading (α) was found to be 0.92 mol CO_2/mol amine at T = 315.65 K, P_{CO2} = 17.73 kPa, m_{TETA} = 0.13 and C = 1 mol/L. This result concluded that optimum equilibrium CO_2 loading could be achieved at low temperature and solution concentration, as well as high values of mole fraction of TETA and partial pressure of CO_2. An empirical model was developed to authenticate the results, and a reliable percentage absolute average relative deviation (% AARD) was found to be 5.631%. The desorption behavior of the aqueous amine blend of TETA+DMAE was performed at a constant temperature and pressure of 393.15 K and 17.73 kPa, respectively. The cyclic equilibrium CO_2 loading and cyclic capacity were estimated in the desorption section. The cyclic loading capacity of the 3 mol/L of the aqueous amine blend of TETA+DMAE was 55.03% higher than 30 wt% (i.e., 5 mol/L) conventional MEA. The heat of CO_2 absorption was estimated with the help of the Gibbs-Helmholtz equation, and for the current aqueous amine blend of TETA+DMAE, it was found to be -67.135 kJ/mol.

This value was lower than that of tertiary amines but higher than that of primary amines, and this indicates that this blend has a good potential for CO_2 capturing.

The availability of the chemical species before and after CO_2 loading was investigated using ^{13}C NMR spectroscopy. A series of chemical reactions were used to demonstrate the reaction chemistry of the TETA+DMAE+CO_2 system, and their authentication was done by NMR spectroscopy. TETA and DMAE peaks were found in CO_2-unloaded amine blend samples at 40.08–49.79 ppm and 60.67–61.96 ppm, respectively. At the same time, the CO_2-loaded amine blend showed the abundance of $TETAH^+$ and $DMAEH^+$ peaks in 40.70–49.84 ppm and 60.70–61.47 ppm, respectively. Finally, the optimization was done with the help of RSM software, it provided F-value of 16.75, R-square value = 0.9399, adjusted R-square value = 0.8838, predicted R-square value = 0.6746, adequate precision = 17.393 and coefficient of variance = 4.70 %. All these values were within the acceptable range, confirming the validity of the experiment. RSM software predicted optimum equilibrium CO_2 loading of 0.926207 mol CO_2/mol amine at T = 304.36 K, m_{TETA} = 0.14, C = 1 mol/L, and P_{CO2} = 17.24 kPa. Finally, the absorption and desorption study on an aqueous amine blend of TETA+DMAE showed good results for the CO_2 capture system. Therefore, this novel amine blend could be recommended to be accepted by the chemical industries to capture CO_2.

ASSOCIATED CONTENT

Appendix – A

Figure A10 to Figure A12, related to this chapter, can be found in Appendix–A.

Table B15 and Table B21**,** related to this chapter, can be found in Appendix–B.

References

[1] Muchan P, Saiwan C, Narku-Tetteh J, Idem R, Supap T, Tontiwachwuthikul P. Screening tests of aqueous alkanolamine solutions based on primary, secondary, and tertiary structure for blended aqueous amine solution selection in post combustion CO_2 capture. Chem Eng Sci 2017;170:574-82. https://doi.org/10.1016/j.ces.2017.02.031

[2] Pandey D, Mondal MK. Thermodynamic modeling and new experimental CO_2 solubility into aqueous EAE and AEEA blend, heat of absorption, cyclic absorption capacity and desorption study for post-combustion CO_2 capture. Chem Eng J. 2021;410:128334. https://doi.org/10.1016/j.cej.2020.128334

[3] Hoyos LA, Paviotti MA, Faroldi BM, Cornaglia LM. Coupling of CO_2 capture and methanation processes using catalysts based on silica recovered from rice husks. Fuel. 2022;324:124604. https://doi.org/10.1016/j.fuel.2022.124604

[4] Chowdhury FA, Okabe H, Shimizu S, Onoda M, Fujioka Y. Development of novel tertiary amine absorbents for CO_2 capture. Energy Procedia 2009;1:1241-8. https://doi.org/10.1016/j.egypro.2009.01.163

[5] Ling H, Gao H, Liang Z. Comprehensive solubility of N_2O and mass transfer studies on an effective reactive N, N-dimethylethanolamine (DMEA) solvent for post-combustion CO_2 capture. Chem Eng J 2019;355:369-79. https://doi.org/10.1016/j.cej.2018.08.147

[6] Sharif M, Zhang T, Wu X, Yu Y, Zhang Z. Evaluation of CO_2 absorption performance by molecular dynamic simulation for mixed secondary and tertiary amines. Int J Greenh Gas Control. 2020;97:103059. https://doi.org/10.1016/j.ijggc.2020.103059

[7] Zhang J, Agar DW, Zhang X, Geuzebroek F. CO_2 absorption in biphasic solvents with enhanced low temperature solvent regeneration. Energy Procedia 2011;4:67-74. https://doi.org/10.1016/j.egypro.2011.01.024

[8] Kumar S, Mondal MK. Equilibrium solubility of CO_2 in aqueous blend of 2-(diethylamine) ethanol and 2-(2-aminoethylamine) ethanol. J Chem Eng Data 2018;63:1163-9. https://doi.org/10.1021/acs.jced.7b00544

[9] Kumar S, Mondal MK. Equilibrium solubility of CO_2 in aqueous binary mixture of 2-(diethylamine) ethanol and 1, 6-hexamethyldiamine. Korean J Chem Eng 2018;35:1335-40. https://doi.org/10.1007/s11814-018-0044-6

[10] Pandey D, Mondal MK. Equilibrium CO_2 solubility in the aqueous mixture of MAE and AEEA: Experimental study and development of modified thermodynamic model. Fluid Ph Equilibria. 2020;522:112766. https://doi.org/10.1016/j.fluid.2020.112766

[11] Singh S, Pandey D, Mondal MK. New Experimental Data on Equilibrium CO_2 Loading into Aqueous 3-Dimethyl Amino-1-propanol and 1, 5-Diamino-2-methylpentane Blend: Empirical Model and CO_2 Absorption Enthalpy. J Chem Eng Data 2020;66:740-8. https://doi.org/10.1021/acs.jced.0c00851

[12] Sreedhar I, Nahar T, Venugopal A, Srinivas B. Carbon capture by absorption–Path covered and ahead. Renew Sustain energy rev 2017;76:1080-107. https://doi.org/10.1016/j.rser.2017.03.109

[13] Kumar S, Mondal MK. Selection of efficient absorbent for CO_2 capture from gases containing low CO_2. Korean J Chem Eng 2020;37:231-9. https://doi.org/10.1007/s11814-019-0440-6

[14] Liu F, Fang M, Dong W, Wang T, Xia Z, Wang Q, Luo Z. Carbon dioxide absorption in aqueous alkanolamine blends for biphasic solvents screening and evaluation. Appl Energy 2019;233:468-77. https://doi.org/10.1016/j.apenergy.2018.10.007

[15] El Hadri N, Quang DV, Goetheer EL, Zahra MR. Aqueous amine solution characterization for post-combustion CO_2 capture process. Appl Energy 2017;185:1433-49. https://doi.org/10.1016/j.apenergy.2016.03.043

[16] Guo H, Li C, Shi X, Li H, Shen S. Non-aqueous amine-based absorbents for energy efficient CO_2 capture. Appl Energy 2019;239:725-34. https://doi.org/10.1016/j.apenergy.2019.02.019

[17] Pandey D, Mondal MK. Experimental data and modeling for viscosity and refractive index of aqueous mixtures with 2-(methylamino) ethanol (MAE) and aminoethylethanolamine (AEEA). J Chem Eng Data 2019;64:3346-55. https://doi.org/10.1021/acs.jced.9b00171

[18] Ahmed RE, Wiheeb AD. Enhancement of carbon dioxide absorption into aqueous potassium carbonate by adding amino acid salts. Mater Today: Proc 2020;20:611-6. https://doi.org/10.1016/j.matpr.2019.09.198

[19] Gervasi J, Dubois L, Thomas D. Screening tests of new hybrid solvents for the post-combustion CO_2 capture process by chemical absorption. Energy Procedia 2014;63:1854-62. https://doi.org/10.1016/j.egypro.2014.11.193

[20] Nwaoha C, Saiwan C, Supap T, Idem R, Tontiwachwuthikul P, Rongwong W, Al-Marri MJ, Benamor A. Carbon dioxide (CO_2) capture performance of aqueous tri-solvent blends containing 2-amino-2-methyl-1-propanol (AMP) and methyldiethanolamine

(MDEA) promoted by diethylenetriamine (DETA). Int J Greenh Gas Control 2016;53:292-04. https://doi.org/10.1016/j.ijggc.2016.08.012

[21] Cao F, Gao H, Xiong Q, Liang Z. Experimental studies on mass transfer performance for CO_2 absorption into aqueous N, N-dimethylethanolamine (DMEA) based solutions in a PTFE hollow fiber membrane contactor. Int J Greenh Gas Control 2019;82:210-7. https://doi.org/10.1016/j.ijggc.2018.12.011

[22] Zhang P, Xu R, Li H, Gao H, Liang Z. Mass transfer performance for CO_2 absorption into aqueous blended DMEA/MEA solution with optimized molar ratio in a hollow fiber membrane contactor. Sep Purif Technol 2019;211:628-36. https://doi.org/10.1016/j.seppur.2018.10.034

[23] Shen Y, Chen H, Wang J, Zhang S, Jiang C, Ye J, Wang L, Chen J. Two-stage interaction performance of CO_2 absorption into biphasic solvents: Mechanism analysis, quantum calculation and energy consumption. Appl Energy. 2020;260:114343. https://doi.org/10.1016/j.apenergy.2019.114343

[24] Zhang J, Qiao Y, Wang W, Misch R, Hussain K, Agar DW. Development of an energy-efficient CO_2 capture process using thermomorphic biphasic solvents. Energy Procedia 2013;37:1254-61. https://doi.org/10.1016/j.egypro.2013.05.224

[25] Xiao M, Cui D, Liu H, Tontiwachwuthikul P, Liang Z. A new model for correlation and prediction of equilibrium CO_2 solubility in N- methyl- 4- piperidinol solvent. AIChE J 2017;63:3395-403. https://doi.org/10.1002/aic.15709

[26] Kim YE, Park JH, Yun SH, Nam SC, Jeong SK, Yoon YI. Carbon dioxide absorption using a phase transitional alkanolamine–alcohol mixture. J Ind Eng Chem 2014;20:1486-92. https://doi.org/10.1016/j.jiec.2013.07.036

[27] Mofarahi M, Khojasteh Y, Khaledi H, Farahnak A. Design of CO_2 absorption plant for recovery of CO_2 from flue gases of gas turbine. Energy 2008;33:1311-9. https://doi.org/10.1016/j.energy.2008.02.013

[28] Conway W, Bruggink S, Beyad Y, Luo W, Melián-Cabrera I, Puxty G, Feron P. CO_2 absorption into aqueous amine blended solutions containing monoethanolamine (MEA), N, N-dimethylethanolamine (DMEA), N, N-diethylethanolamine (DEEA) and 2-amino-2-methyl-1-propanol (AMP) for post-combustion capture processes. Chem Eng Sci 2015;126:446-54. https://doi.org/10.1016/j.ces.2014.12.053

[29] Luo X, Fu K, Yang Z, Gao H, Rongwong W, Liang Z, Tontiwachwuthikul P. Experimental studies of reboiler heat duty for CO_2 desorption from triethylenetetramine (TETA) and triethylenetetramine (TETA) + N-methyldiethanolamine (MDEA). Ind Eng Chem Res 2015;54:8554-60. https://doi.org/10.1021/acs.iecr.5b00158

[30] Quan C, Chu H, Zhou Y, Su S, Su R, Gao N. Amine-modified silica zeolite from coal gangue for CO_2 capture. Fuel. 2022;322:124184. https://doi.org/10.1016/j.fuel.2022.124184

[31] Liu F, Jing G, Zhou X, Lv B, Zhou Z. Performance and mechanisms of triethylene tetramine (TETA) and 2-amino-2-methyl-1-propanol (AMP) in aqueous and non-aqueous solutions for CO_2 capture. ACS Sustain Chem Eng 2018;6:1352-61. https://doi.org/10.1021/acssuschemeng.7b03717

[32] Ramezani R, Mazinani S, Di Felice R. Experimental Study of CO Absorption in Potassium Carbonate Solution Promoted by Triethylenetetramine. Open Chem Eng J 2018;12:67-79. 10.2174/1874123101812010067

[33] Schäffer A, Brechtel K, Scheffknecht G. Comparative study on differently concentrated aqueous solutions of MEA and TETA for CO_2 capture from flue gases. Fuel 2012;101:148-53. https://doi.org/10.1016/j.fuel.2011.06.037

[34] Tzirakis F, Papadopoulos AI, Seferlis P, Tsivintzelis I. CO_2 Solubility in diethylenetriamine (DETA) and triethylenetetramine (TETA) aqueous mixtures: Experimental investigation and correlation using the CPA equation of state. Chem Thermody Therm Analysis. 2021;3:100017. https://doi.org/10.1016/j.ctta.2021.100017

[35] Wang M, Rao N, Liu Y, Li J, Cheng Q, Li J. Enhancement of CO_2 capture in the MDEA solution by introducing TETA or TETA-AEP mixtures as an activator. Sep Sci Technol 2019;54:101-9. https://doi.org/10.1080/01496395.2018.1504797

[36] Zheng S, Tao M, Liu Q, Ning L, He Y, Shi Y. Capturing CO_2 into the precipitate of a phase-changing solvent after absorption. Environ Sci Technol 2014;48:8905-10. https://doi.org/10.1021/es501554h

[37] Kortunov PV, Siskin M, Baugh LS, Calabro DC. In situ nuclear magnetic resonance mechanistic studies of carbon dioxide reactions with liquid amines in aqueous systems: New insights on carbon capture reaction pathways. Energy Fuels 2015;29:5919-39. https://doi.org/10.1021/acs.energyfuels.5b00850

[38] Barzagli F, Mani F, Peruzzini M. Novel water-free biphasic absorbents for efficient CO_2 capture. Int J Greenh Gas Control 2017;60:100-9. https://doi.org/10.1016/j.ijggc.2017.03.010

[39] Wang W, Peng Z, Gao H, Sema T, Shi J, Liang Z. New insight and evaluation of secondary Amine/N-butanol biphasic solutions for CO_2 Capture: Equilibrium Solubility,

phase separation behavior, absorption Rate, desorption Rate, energy consumption and ion species. Chem Eng J. 2022;431:133912. https://doi.org/10.1016/j.cej.2021.133912

[40] Longeras O, Gautier A, Ballerat-Busserolles K, Andanson JM. Tuning critical solution temperature for CO_2 capture by aqueous solution of amine. J Mol Liq. 2021;343:117628. https://doi.org/10.1016/j.molliq.2021.117628

[41] Lv J, Liu S, Ling H, Gao H, Olson W, Li Q, Bairq ZA, Liang Z. Development of a Promising Biphasic Absorbent for Post combustion CO_2 Capture: Sulfolane + 2-(Methylamino) ethanol + H_2O. Ind Eng Chem Res. 2020;59:14496-06. https://doi.org/10.1021/acs.iecr.0c02389

[42] Wang R, Liu S, Wang L, Li Q, Zhang S, Chen B, Jiang L, Zhang Y. Superior energy-saving splitter in monoethanolamine-based biphasic solvents for CO_2 capture from coal-fired flue gas. Appl Energy 2019;242:302-10. https://doi.org/10.1016/j.apenergy.2019.03.138

[43] Alkhatib III , Galindo A, Vega LF. Systematic study of the effect of the co-solvent on the performance of amine-based solvents for CO_2 capture. Sep Purif Technol. 2022;282:120093. https://doi.org/10.1016/j.seppur.2021.120093

[44] Xu Z, Wang S, Chen C. CO_2 absorption by biphasic solvents: Mixtures of 1, 4-Butanediamine and 2-(Diethylamino)-ethanol. Int J Greenh Gas Control 2013;16:107-15. https://doi.org/10.1016/j.ijggc.2013.03.013

[45] Liang ZH, Rongwong W, Liu H, Fu K, Gao H, Cao F, Zhang R, Sema T, Henni A, Sumon K, Nath D. Recent progress and new developments in post-combustion carbon-capture technology with amine based solvents. Int J Greenh Gas Control 2015;40:26-54. https://doi.org/10.1016/j.ijggc.2015.06.017

[46] Nuchitprasittichai A, Cremaschi S. Optimization of CO_2 Capture Process with Aqueous Amines- A Comparison of Two Simulation–Optimization Approaches. Ind Eng Chem Res 2013;52:10236-43. https://doi.org/10.1021/ie3029366

[47] Garcia S, Gil MV, Martín CF, Pis JJ, Rubiera F, Pevida C. Breakthrough adsorption study of a commercial activated carbon for pre-combustion CO_2 capture. Chem Eng J 2011;171:549-56. https://doi.org/10.1016/j.cej.2011.04.027

[48] Tang Q, Lau YB, Hu S, Yan W, Yang Y, Chen T. Response surface methodology using Gaussian processes: Towards optimizing the trans-stilbene epoxidation over Co^{2+}–NaX catalysts. Chem Eng J 2010;156:423-31. https://doi.org/10.1016/j.cej.2009.11.002

[49] Sahraie S, Rashidi H, Valeh-e-Sheyda P. An optimization framework to investigate the CO_2 capture performance by MEA: Experimental and statistical studies using Box-Behnken design. Process Saf Environ Prot 2019;122:161-8. https://doi.org/10.1016/j.psep.2018.11.026

[50] Hemmati A, Rashidi H, Hemmati A, Kazemi A. Using rate based simulation, sensitivity analysis and response surface methodology for optimization of an industrial CO_2 capture plant. J Nat Gas Sci Eng 2019;62:101-12. https://doi.org/10.1016/j.jngse.2018.12.002

[51] Nuchitprasittichai A, Cremaschi S. Optimization of CO_2 capture process with aqueous amines using response surface methodology. Comput Chem Eng 2011;35:1521-31. https://doi.org/10.1016/j.compchemeng.2011.03.016

[52] Gil MV, Martínez M, Garcia S, Rubiera F, Pis JJ, Pevida C. Response surface methodology as an efficient tool for optimizing carbon adsorbents for CO_2 capture. Fuel Process Technol 2013;106:55-61. https://doi.org/10.1016/j.fuproc.2012.06.018

[53] Song C, Kitamura Y, Li S. Optimization of a novel cryogenic CO_2 capture process by response surface methodology (RSM). J Taiwan Inst Chem Eng 2014;45:1666-76. https://doi.org/10.1016/j.jtice.2013.12.009

[54] Das D, Meikap BC. Optimization of process condition for the preparation of amine-impregnated activated carbon developed for CO_2 capture and applied to methylene blue adsorption by response surface methodology. J Environ Sci Health 2017;52:1164-72. https://doi.org/10.1080/10934529.2017.1356204

[55] Saeidi M, Ghaemi A, Tahvildari K, Derakhshi P. Exploiting response surface methodology (RSM) as a novel approach for the optimization of carbon dioxide adsorption by dry sodium hydroxide. J Chin Chem Soc 2018;65:1465-75. https://doi.org/10.1002/jccs.201800012

[56] Asgarifard P, Rahimi M, Tafreshi N. Response surface modelling of CO_2 capture by ammonia aqueous solution in a microchannel. Can J Chem Eng 2021;99:601-12. https://doi.org/10.1002/cjce.23881

[57] Gao H, Wu Z, Liu H, Luo X, Liang Z. Experimental studies on the effect of tertiary amine promoters in aqueous monoethanolamine (MEA) solutions on the absorption/stripping performances in post-combustion CO_2 capture. Energy fuels 2017;31:13883-91. https://doi.org/10.1021/acs.energyfuels.7b02390

[58] Rho SW, Yoo KP, Lee JS, Nam SC, Son JE, Min BM. Solubility of CO_2 in aqueous methyldiethanolamine solutions. J Chem Eng Data 1997;42:1161-4. https://doi.org/10.1021/je970097d

[59] Kim I, Svendsen HF. Heat of absorption of carbon dioxide (CO_2) in monoethanolamine (MEA) and 2-(aminoethyl) ethanolamine (AEEA) solutions. Ind Eng Chem Res 2007;46:5803-9. https://doi.org/10.1021/ie0616489

[60] Mathias PM, O'Connell JP. The Gibbs–Helmholtz equation and the thermodynamic consistency of chemical absorption data. Ind Eng Chem Res 2012;51:5090-7. https://doi.org/10.1021/ie202668k

[61] Caplow M. Kinetics of carbamate formation and breakdown. J Am Chem Soc 1968;90:6795-803. https://doi.org/10.1021/ja01026a041

[62] Danckwerts PV. The reaction of CO_2 with ethanolamines. Chem Eng Sci 1979;34:443-6. https://doi.org/10.1016/0009-2509(79)85087-3

[63] Donaldson TL, Nguyen YN. Carbon dioxide reaction kinetics and transport in aqueous amine membranes. Ind Eng Chem Fundam 1980;19:260-6. https://doi.org/10.1021/i160075a005

[64] Perinu C, Arstad B, Jens KJ. NMR spectroscopy applied to amine–CO_2–H_2O systems relevant for post-combustion CO_2 capture: A review. Int J Greenh Gas Control 2014;20:230-43. https://doi.org/10.1016/j.ijggc.2013.10.029

[65] Zhang R, Jiang W, Liang Z, Luo X, Yang Q. Study of equilibrium solubility, heat of absorption, and speciation of CO_2 absorption into aqueous 2-methylpiperazine (2MPZ) solution. Ind Eng Chem Res 2018;57:17496-503. https://doi.org/10.1021/acs.iecr.8b03104

[66] Zheng W, Yan Z, Zhang R, Jiang W, Luo X, Liang Z, Yang Q, Yu H. A study of kinetics, equilibrium solubility, speciation and thermodynamics of CO_2 absorption into benzylamine (BZA) solution. Chem Eng Sci. 2022;251:117452. https://doi.org/10.1016/j.ces.2022.117452